

NRL Report 6172

**The Computation of Optimum Orbital
Elements Derived From a Single
Coincident Observation by Two
Receiving Stations of the Naval
Space Surveillance System**

H. G. DEVEZIN, JR.

*Space Surveillance Branch
Applications Research Division*

October 22, 1964



**U.S. NAVAL RESEARCH LABORATORY
Washington, D.C.**

ACKNOWLEDGMENTS

I would like to thank the Naval Research Laboratory for permission to use as thesis material work done at the laboratory. Particularly I am grateful to my immediate supervisor Mr. Donald W. Lynch for his encouragement and helpful criticism of the manuscript, to Mr. C. A. Bartholomew who designed and set up the equipment used in the measurement of doppler shift, and to Dr. Herbert A. Hauptman for his guidance in the preparation of the thesis. Thanks are also due to Mr. James A. Buisson, III, and Mr. Bernard Kaufman for their assistance in proofreading and to Mrs. Emily I. Balacek for her capable typing of the manuscript and final copy.

THE COMPUTATION OF OPTIMUM ORBITAL ELEMENTS DERIVED FROM
A SINGLE COINCIDENT OBSERVATION BY TWO RECEIVING STATIONS OF
THE NAVAL SPACE SURVEILLANCE SYSTEM

by

Howard Gerard deVezin, Jr.

Thesis submitted to the Faculty of the Graduate School
of the University of Maryland in partial fulfillment
of the requirements for the degree of
Master of Science
1964

UNIVERSITY OF MARYLAND

ABSTRACT

Title of Thesis: The Computation of Optimum Orbital Elements Derived from a Single Coincident Observation by Two Receiving Stations of the Naval Space Surveillance System

Howard G. deVezin, Jr., Master of Science, 1964

Thesis directed by: Dr. Herbert A. Hauptman

This thesis is concerned with an investigation into a method of determining the orbital elements of a passive artificial earth satellite using information obtained from a single coincident satellite observation of short time duration. This information is obtained from two receiving stations of the U.S. Naval Space Surveillance System, a C.W. radar network of three transmitting stations and four receiving stations which sets up an electronic "fence" stretching across the southern United States.

A list of the information given by two receiving stations is as follows: two east-west angles (angles measured in the plane of the detection "fence"), two north-south angles (angles measured normal to the plane of the detection "fence"), rate of change of east-west direction cosine measured by both stations, and rate of change of north-south direction cosine measured by both stations. In addition the system can be adapted to measure the doppler frequency shift from one of the three transmitters to the receiver station and the distance from one of the three transmitters to the satellite to the receiver station (bi-static range).

All of this information results in redundant data (i.e. more data than are needed to determine the orbit of the satellite). In addition, owing to inaccuracies of the system and owing to noise, different groupings of the information will produce different values of orbital parameters; hence in general the information is inconsistent.

The purpose of this thesis is to arrive at a method of computing orbital elements using all of the information that the system does measure or can be adapted to measure. This method would introduce weighting factors determined, for example, by the accuracy with which the system can measure the parameter in question. This method is then used to study the effect that the addition of doppler shift and bistatic range measurements have on the accuracy of the resulting orbital elements.

PROBLEM STATUS

This is an interim report on a continuing problem.

AUTHORIZATION

NRL Problem R02-35
BuWeps Project RT 8801-001/652-1/S434-00-01

Manuscript submitted September 8, 1964.

TABLE OF CONTENTS

Chapter	Page
I. THE SPACE SURVEILLANCE SYSTEM	1
A. Historical Background	1
B. Theory of Detection	2
C. Single Pass Orbits	7
II. METHOD OF ELEMENT COMPUTATION	12
A. Use of Redundant Data	12
B. Position Determination	13
C. Velocity Determination	23
D. Determination of Classical Elements	27
III. ERROR ANALYSIS	35
A. Method of Error Determination	35
B. Dependence of Errors on Accuracy of Measured Doppler Shift	40
C. Dependence of Errors on Accuracy of Measured Range	44
IV. EXPERIMENTAL RESULTS	50
APPENDIX A	61
SELECTED BIBLIOGRAPHY	66

LIST OF TABLES

Table	Page
I. Comparison Between Classical Orbital Elements Derived from Data Runs 1-10, Computed for Doppler Shift Sigma Values of 10 and 10^{21} c.p.s., and Differentially Corrected Elements	52
II. Cross Track Error in Miles Computed from Data Runs 1-10 with Doppler Shift Measurement Not Included in the Computations (Case I), and R.M.S. Values Computed for Indicated Central Angles	54
III. Height Error in Miles Computed from Data Runs 1-10 with Doppler Shift Measurement Not Included in the Computations (Case I), and R.M.S. Values Computed for Indicated Central Angles	55
IV. Time Error in Seconds Computed from Data Runs 1-10 with Doppler Shift Measurement Not Included in the Computations (Case I), and R.M.S. Values Computed for Indicated Central Angles	55
V. Cross Track Error in Miles Computed from Data Runs 1-10 with Doppler Shift Measurement Included in the Computations (Case II), and R.M.S. Values Computed for Indicated Central Angles	56
VI. Height Error in Miles Computed from Data Runs 1-10 with Doppler Shift Measurement Included in the Computations (Case II), and R.M.S. Values Computed for Indicated Central Angles	56
VII. Time Error in Seconds Computed from Data Runs 1-10 with Doppler Shift Measurement Included in the Computations (Case II), and R.M.S. Values Computed for Indicated Central Angles	57

LIST OF FIGURES

Figure	Page
1. Space Surveillance Station Complex	3
2. Interferometer Receiving Signal	3
3. Station Parameters	6
4. Two Point Orbit	9
5. Approximate Satellite Position	16
6. Right Ascension of the Ascending Node	30
7. Sum of Anomaly and Argument of Perigee in \bar{x}, \bar{y} Plane	33
8. Representation of Error Plane at Central Angle θ	37
9. Distance from P_2 to the Error Plane	39
10. Representation of Errors Δx and Δh	41
11. Relation Between R.S.S. Cross Track Error and Central Angle	46
12. Relation Between R.S.S. Height Error and Central Angle	47
13. Relation Between R.S.S. Time Error and Central Angle	48
14. Relation Between ΔR_{RSS} and Central Angle	49
15. Relation Between Experimental R.M.S. Cross Track Error and Central Angle for Case I and Case II	58
16. Relation Between Experimental R.M.S. Height Error and Central Angle for Case I and Case II	59
17. Relation Between Experimental R.M.S. Time Error and Central Angle for Case I and Case II	60

CHAPTER I

THE SPACE SURVEILLANCE SYSTEM

Historical Background

The U. S. Naval Space Surveillance System consists of a network of CW transmitting stations and receiving stations stretching across the Southern portion of the United States. In addition the system includes data transmission lines, a data reduction center located at the Naval Weapons Laboratory at Dahlgren, Virginia, and a high speed computer used for the calculation of satellite orbits and predictions, making the system a complete one for satellite detection, identification, and prediction.

The major purpose of the system is to detect and maintain a surveillance on passive, non-radiating satellites. It was for this reason that the Advanced Research Projects Agency, on June 20, 1958, authorized the Naval Research Laboratory to develop, install, and operate such a system.¹ Six weeks later a two-station facility was in operation with a transmitter at Jordan Lake, Alabama, and a receiver at Ft. Stewart, Georgia.

The first signal to be received simultaneously by two receiver stations was transmitted on December 22, 1958. The second receiver was located at Silver Lake, Mississippi, which lies about 250 miles west of the Jordan Lake transmitter. Although, owing to calibration errors, these early data were not entirely correct, the calibration problems were eventually overcome and by February, 1959, the network had grown

to include four receiver stations and two 50-KW transmitting stations and was operating on a twenty-four-hour-per-day basis. In June, 1961, the range and coverage of the system were significantly increased by the installation of the 560-KW CW transmitter located at Lake Kickapoo, Texas. The other two receiver stations are located at San Diego, California, and Elephant Butte, Arizona, and the other transmitter is located at Gila River, New Mexico.

Theory of Detection

A typical transmitting antenna in the system consists of a long linear array of dipole antennas which produce illumination in a narrow fan beam which is coplanar with the similar antenna patterns of the receiver stations.² As a satellite passes through this electromagnetic "fence", whose thickness is about 0.3 degrees, the signal from the transmitter is reflected to one or more of the receiving stations. Two angles, one in the plane of the fence and one normal to the plane of the fence, are measured at a receiving station by means of interferometers. These data from two receiving stations provide a triangulation which defines the satellite position in space at the time of observation. The station complex of the system together with a coincident passive satellite observation is shown in Figure 1, where R and T indicate receiving stations and transmitting stations respectively.

The method of obtaining angle using an interferometer can be seen from Figure 2 together with the following equation:

$$\cos \theta = \frac{\Delta l}{b_\lambda} \quad (1)$$

where b_λ is the baseline length expressed in wavelengths, and Δl is the phase difference in wavelengths. The accuracy of measured angle

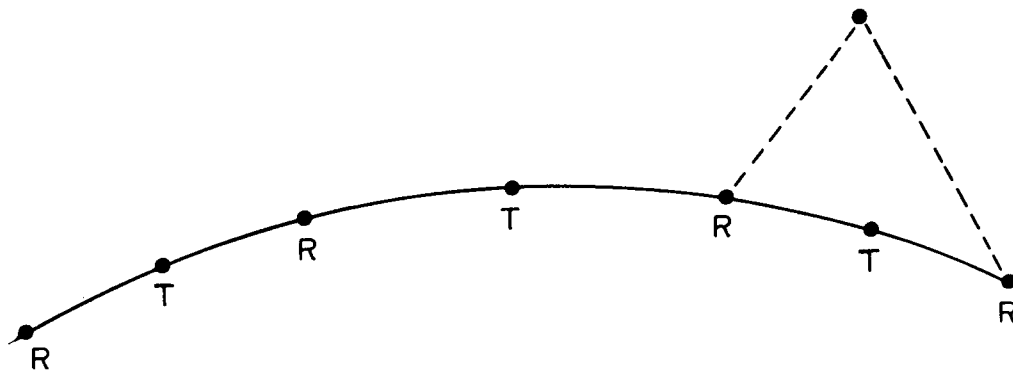


Figure 1 - Space Surveillance Station Complex

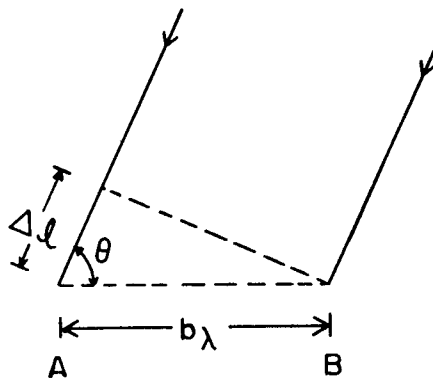


Figure 2 - Interferometer Receiving Signal

increases with baseline length. However, for long baselines Δl is of the form $n + \Delta\phi$ where n is an integral number of wavelengths and $\Delta\phi$ is the phase difference in fractions of a wavelength. $\Delta\phi$ can be measured directly but n cannot be measured by one long baseline and shorter baselines are needed so that the ambiguity can be eliminated. Hence an interferometer system will in general contain several baselines of varying length. In the Space Surveillance system they vary from a 16-foot baseline to a 5200-foot baseline. We can therefore think of the system as measuring the direction cosine of the incoming signal relative to a vector from antenna A to antenna B both located at the same receiver. Each receiver station is set up with two such interferometers. One is shown in Figure 2 with its vector lying in the plane of the detection "fence" from antenna A to antenna B and measuring the angle between this vector and the line from antenna A to the satellite. This angle is measured in an east-west direction, and is called "east-west" angle. The second interferometer has its vector lying normal to the detection fence, along antenna A and measuring angle in a north-south direction. For a given satellite observation these two measurements define the direction of the position vector from the station to the satellite. The vector from antenna to antenna will be designated as vector \vec{u} , and the vector along the antenna will be designated as \vec{v} . These vectors along with the position of the station expressed in a given coordinate system comprise all of the required station information for the calculations in this paper. The coordinate system chosen is a right-handed rectangular one fixed in the earth with the origin at the center of the earth, the x-axis going through 0° longitude, the z-axis going through the north pole, and the y-axis through 90° east

longitude. The station parameters are illustrated in Figure 3, with two stations denoted by subscripts 1 and 2, a transmitter at T and a satellite located at point (x,y,z). The vector from the center of the earth to the satellite is \vec{R} , and \vec{R}_1 , \vec{R}_2 and \vec{R}_T are the vectors from the center of the earth to receiver stations 1 and 2 and the transmitter respectively.

In addition to direction cosines measured in an east-west and north-south direction, the system also measures rate of change of these direction cosines. From the output information received from the interferometer, rate of change of phase can be computed by measuring the phase at two times and dividing by the time difference. This gives us an approximation to $\frac{d}{dt} \Delta l$ which can be inserted into the derivative of equation (1)

$$\frac{d}{dt} (\cos \theta) = \frac{1}{b_\lambda} \frac{d}{dt} (\Delta l) \quad (2)$$

to obtain the rate of change of direction cosine.

With additional equipment, the system can be adapted to measure the doppler frequency shift which is defined as the difference between transmitted and received signal frequency. This frequency shift is due to the fact that the path of the signal from transmitter to satellite to receiver is changing with time. The doppler shift can be obtained by measuring the frequency of the incoming signal and subtracting from this value the frequency of the transmitted signal (108.015 Mc). However, because of the thinness of the fence beam, a 1000-mile-high satellite having a high inclination will be in the beam for approximately one second. This narrow beamwidth reduces the accuracy of the measured doppler shift because of the short time period of observation. Since the present operational system is not equipped to measure doppler shift, additional electronic equipment had to be installed at the receiving

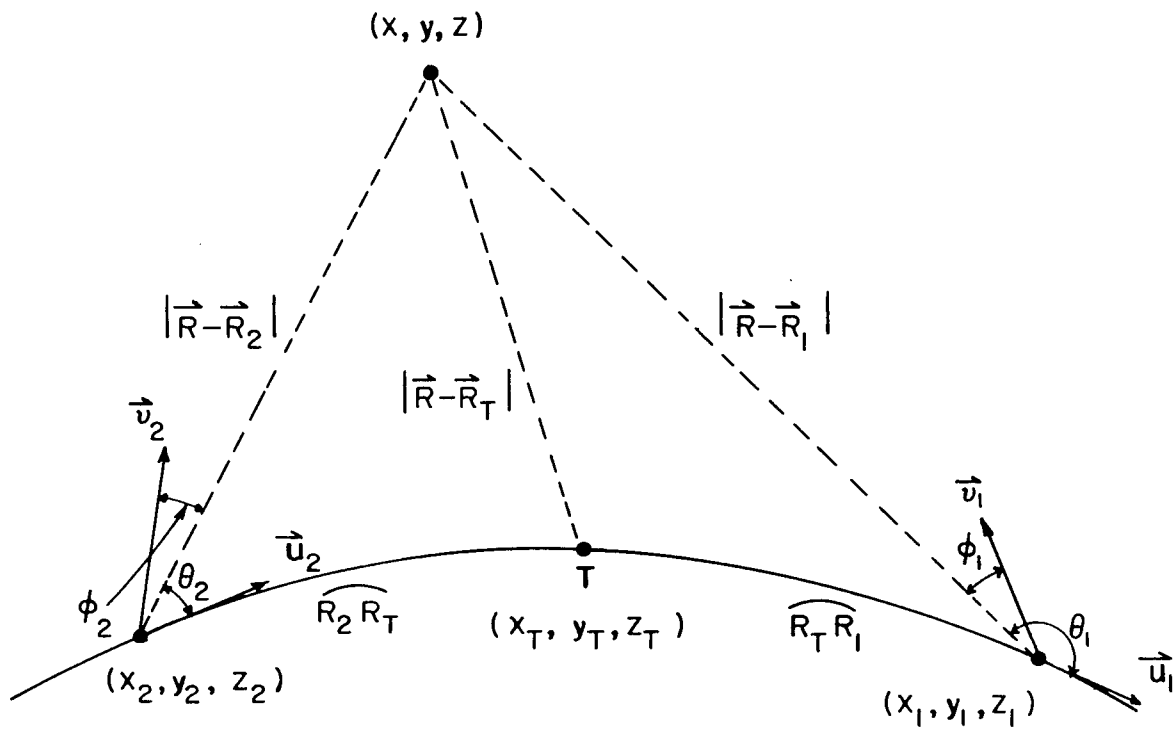


Figure 3 - Station Parameters

stations to acquire the doppler data for the experimental results described below. The system can also be adapted to measure bi-static range. This is defined as the difference between the distance from the transmitter to the satellite to the receiver, and the distance from the transmitter to the receiver along the surface of the earth. In Figure 3 the bi-static range measured at station 1 would be

$$|\vec{R} - \vec{R}_T| + |\vec{R} - \vec{R}_1| - \widehat{R_T R_1}.$$

Owing to the high cost involved, it was not possible to set up a range measuring experiment as was done with doppler. However, range is included in the analysis below and its influence on the accuracy of resulting orbital elements is studied.

Single Pass Orbits

In the Space Surveillance System there are two objectives which dictate the method to be used in obtaining the orbital elements from observed data. In the first case very accurate elements are derived from a large amount of data for the purpose of making accurate predictions for a relatively long period of time (i.e. weeks). This method is particularly useful for obtaining predictions of geodetic and communication satellites where the position of the satellite in a given coordinate system must be known precisely. However, a considerable amount of time is needed to acquire the data employed by this method. For example, the system uses data observed over a one-week period in its calculation of differentially corrected elements.

The second of the objectives referred to above is that the elements be obtained in as short a time as possible after the system's first observation of the satellite. An application of this method is to predict future system observations of new objects appearing for the first

time. There are three methods of orbit computation falling into this category and each sacrifices accuracy, to a greater or lesser degree, for speed of element acquisition after observation. The first of these uses as input, two points, each a result of two-station triangulation, which are widely separated on the ellipse. For example in Figure 4, the satellite is detected at point A, then, several revolutions later, the earth has rotated beneath the orbit and the satellite is observed at point B on the orbit. The exact number of revolutions between these observations depends on the period of the satellite in question. These are the two points on the orbit whose projections on the earth are at 33.4° N latitude, the latitude of the detection fence. When the inclination of the orbit with the equatorial plane equals 33.4° these two points degenerate into one, and when the inclination is 90° the angle subtended at the center of the earth between the two points is a maximum.

The elapsed time between these observations is the time required for the earth to rotate the detection fence from point A to point B. This time, for a nominal circular orbit, 1000 miles high and inclined at 50° with the equator, is approximately 6 to 9 hours. This method is called the "two-point" method³ and is considerably more accurate in predicting satellite position than the remaining two methods; however the elapsed time mentioned above is the largest of the three cases and for certain applications this difference can be significant.

A second method is similar to the above mentioned "two-point" orbit, except that the two points are measured on consecutive revolutions of the satellite crossing the detection fence. This results in two points along the orbit which are very close together. The time span from

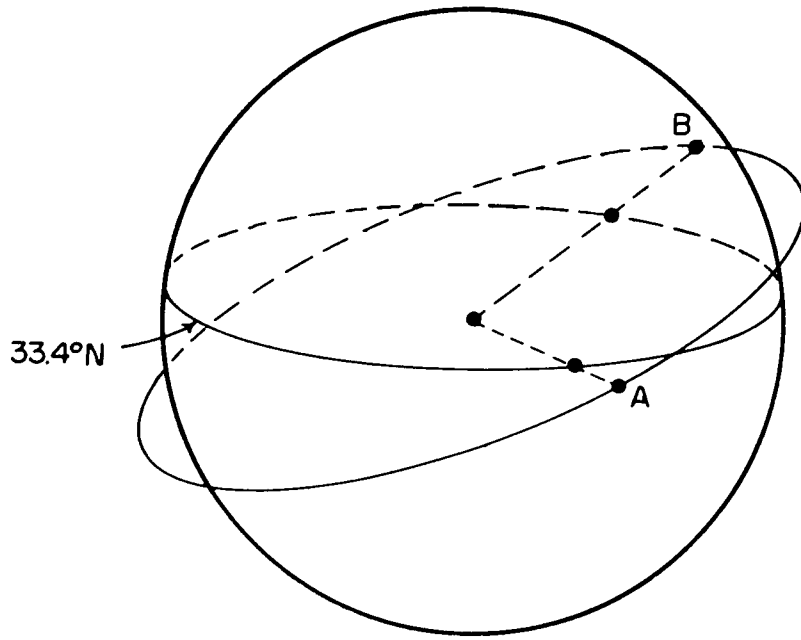


Figure 4 - Two Point Orbit

observation to element acquisition is approximately equal to the period of the satellite, which, for the above nominal orbit, is approximately two hours.

The third method, and the one that we will concern ourselves with below, uses the information obtained from one coincident satellite observation, i.e. a single pass observed by two receiving stations. Unlike the above mentioned methods, velocity must be calculated directly from the observed data. Hence angle information alone is not sufficient, and parameters from which velocity can be directly obtained, e.g. phase-rate and doppler shift, must be introduced.

The detection system was originally designed to measure position accurately. For this reason the angular width of the beam was made as small as possible. This design, however, makes accurate measurement of velocity more difficult. Nevertheless, since velocity information is present, it was decided that a study be made to see if these data could yield useful orbital elements.

The value of such elements can readily be seen from the fact that only with this method could any predictions be made prior to two observations of the satellite. Or, considering our nominal set, we could reduce the time interval needed to obtain predictions from two hours to a matter of seconds. Hence such a method would be particularly useful for purposes of rendezvous as soon as possible after launch.

A method of computing elements from a single satellite pass through the fence was devised by the author and James A. Buisson III, under the supervision of Donald W. Lynch. This method uses a minimum of data consisting of angles and phase-rate from the two receiving stations. However, there exist some applications which require more accurate elements than those produced by this method.

It is the purpose of this study to devise a new method of satellite orbit computation which best uses all available information obtained from one coincident satellite observation, and to determine the usefulness of such a set of elements. This study will also determine to what extent the accuracy of the resulting elements is improved by the introduction of doppler shift and range. This would then serve as a guide to determine whether or not these improvements warrant the expenditures involved in their installation.

It should be pointed out that the measurements involved in this work are derived from experimental runs involving minimum data, and that they do not represent operational system accuracies.

CHAPTER II

METHOD OF ELEMENT COMPUTATION

Use of Redundant Data

A value of satellite position relative to coordinate axes fixed on the earth can be obtained from three independent measurements. Hence a combination of any three values of the two ranges, two east-west angles and one north-south angle observed by two stations during a given satellite pass, can be used to obtain an approximate value for position. Since the observations are made when the satellite is approximately in the detection fence (east-west direction), two measurements of north-south angle (each approximately 90°) would be essentially redundant, and small errors in these measurements would lead to large errors in position. It is for this reason that two of the three input parameters cannot be north-south angles. Similarly a value of velocity in this same earth-fixed coordinate set can be obtained from three measurements. In this case one value of north-south angle rate must be included since, if the measurement is made in the plane of the fence, east-west angle rates and values of doppler frequency measure components of velocity only in the plane of the detection "fence". The north-south angle rate is needed in this case to produce a component of velocity normal to the "fence".

Owing to inaccuracies in the system and to noise, different subsets of the total redundant data will in general yield different values of position and velocity. It is therefore desirable to make use of all the information received and arrive at statistically optimum values of position

and velocity. Such an approach must take into account the accuracy with which individual parameters can be measured. A Gaussian distribution of errors in all measured parameters is assumed. The errors both in the case of position and in the case of velocity are independent of one another and are assumed to be random rather than systematic.

Position Determination

From a given station, the data employed in the determination of satellite position are east-west angle, north-south angle, and bi-static range. These measurements have been discussed in Chapter I. This information received from two receiver stations during a coincident observation results in six input parameters from which the three coordinates are to be computed.

An expression relating east-west angle and satellite position coordinates can be obtained by dotting the vector \vec{u}_i (Chapter I, Figure 3) with the vector from the receiving station to the satellite ($\vec{R} - \vec{R}_i$):

$$\vec{u}_i \cdot (\vec{R} - \vec{R}_i) = |\vec{R} - \vec{R}_i| \cos \theta_i$$

where $i = 1$ for the east receiver station and $i = 2$ for the west receiver station. Putting this into component form we have

$$\cos \theta_i = \frac{u_{ix} (x - x_i) + u_{iy} (y - y_i) + u_{iz} (z - z_i)}{\sqrt{(x - x_i)^2 + (y - y_i)^2 + (z - z_i)^2}} \quad (3)$$

Similarly by using the vector \vec{v}_i we can obtain the following expression relating north-south angle and position coordinates:

$$\cos \phi_i = \frac{v_{ix} (x - x_i) + v_{iy} (y - y_i) + v_{iz} (z - z_i)}{\sqrt{(x - x_i)^2 + (y - y_i)^2 + (z - z_i)^2}} \quad (4)$$

The expression relating bi-static range and satellite coordinates follows from the equation in Chapter I:

$$R_{oi} = |\vec{R} - \vec{R}_T| + |\vec{R} - \vec{R}_i| - \widehat{\vec{R}_T \vec{R}_i} .$$

Upon expanding the vectors into their components we obtain

$$R_{oi} = \sqrt{(x - x_T)^2 + (y - y_T)^2 + (z - z_T)^2} + \sqrt{(x - x_i)^2 + (y - y_i)^2 + (z - z_i)^2} - C_i \quad (5)$$

where: R_{oi} is the calculated bi-static range ($i = 1, 2$); x, y, z are satellite coordinates; x_T, y_T, z_T are transmitter coordinates; x_i, y_i, z_i are receiver station coordinates; and C_i is an approximate value of the distance along the arc from transmitter to receiver:

$$C_i = \left[\frac{|\vec{R}_i| + |\vec{R}_T|}{2} \right] \cos^{-1} \left[\frac{\vec{R}_T \cdot \vec{R}_i}{|\vec{R}_T| |\vec{R}_i|} \right].$$

Equations (3), (4), and (5) represent six equations which can be employed in a least squares sense to obtain the values of satellite position best fitting the measured data.

From the stand-point of ease of solution, it is desirable that these six equations be reduced to six linear equations. To obtain these linear equations one must first obtain approximate expressions for the satellite position coordinates (x', y', z'). These can be found through the use of east-west and north-south angles from both receiver stations.

From Figure 5

$$\vec{R}' = \vec{R}_1 + \vec{S}_1 = \vec{R}_1 + S_1 \cos \theta_{u1} \vec{u}_1 + S_1 \cos \theta_{v1} \vec{v}_1 + S_1 \cos \theta_{w1} \vec{w}_1,$$

where θ_{ui} is the angle from \vec{u}_i to \vec{S}_i , θ_{vi} is the angle from \vec{v}_i to \vec{S}_i , and θ_{wi} is the angle from \vec{w}_i to \vec{S}_i . Putting the above equation into component form we have

$$x'i + y'j + z'k = x_1i + y_1j + z_1k + S_1 \cos \theta_{u1} (u_{1x} i + u_{1y} j + u_{1z} k) + S_1 \cos \theta_{v1} (v_{1x} i + v_{1y} j + v_{1z} k)$$

$$+ S_1 \cos \theta_{w1} (w_{1x} \vec{i} + w_{1y} \vec{j} + w_{1z} \vec{k}) \quad (6)$$

and equating coefficients,

$$x' = x_1 + S_1 (\cos \theta_{u1} u_{1x} + \cos \theta_{v1} v_{1x} + \cos \theta_{w1} w_{1x}).$$

But $R' = R_2 + S_2$; therefore

$$x' = x_2 + S_2 (\cos \theta_{u2} u_{2x} + \cos \theta_{v2} v_{2x} + \cos \theta_{w2} w_{2x}).$$

Let $a_{xi} = \cos \theta_{ui} u_{ix} + \cos \theta_{vi} v_{ix} + \cos \theta_{wi} w_{ix}$;

then we have

$$x' = x_1 + a_{x1} S_1 = x_2 + a_{x2} S_2. \quad (7)$$

Let $a_{yi} = \cos \theta_{ui} u_{iy} + \cos \theta_{vi} v_{iy} + \cos \theta_{wi} w_{iy}$

and $a_{zi} = \cos \theta_{ui} u_{iz} + \cos \theta_{vi} v_{iz} + \cos \theta_{wi} w_{iz}$,

and similarly by equating coefficients of y and z in eq. (6) we obtain:

$$y' = y_1 + a_{y1} S_1 = y_2 + a_{y2} S_2, \quad (8)$$

and

$$z' = z_1 + a_{z1} S_1 = z_2 + a_{z2} S_2. \quad (9)$$

From equation (7)

$$S_1 = \frac{x' - x_1}{a_{x1}} \quad \text{and} \quad S_2 = \frac{x' - x_2}{a_{x2}},$$

and using eq. (8), we have

$$y' = y_1 + a_{y1} \left[\frac{x' - x_1}{a_{x1}} \right] = y_2 + a_{y2} \left[\frac{x' - x_2}{a_{x2}} \right]$$

or

$$\left[\frac{a_{y1}}{a_{x1}} - \frac{a_{y2}}{a_{x2}} \right] x' = (y_2 - y_1) + \frac{a_{y1} x_1}{a_{x1}} - \frac{a_{y2} x_2}{a_{x2}}$$

$$x' = \frac{(y_2 - y_1) + \frac{a_{y1} x_1}{a_{x1}} - \frac{a_{y2} x_2}{a_{x2}}}{\frac{a_{y1}}{a_{x1}} - \frac{a_{y2}}{a_{x2}}}. \quad (10)$$

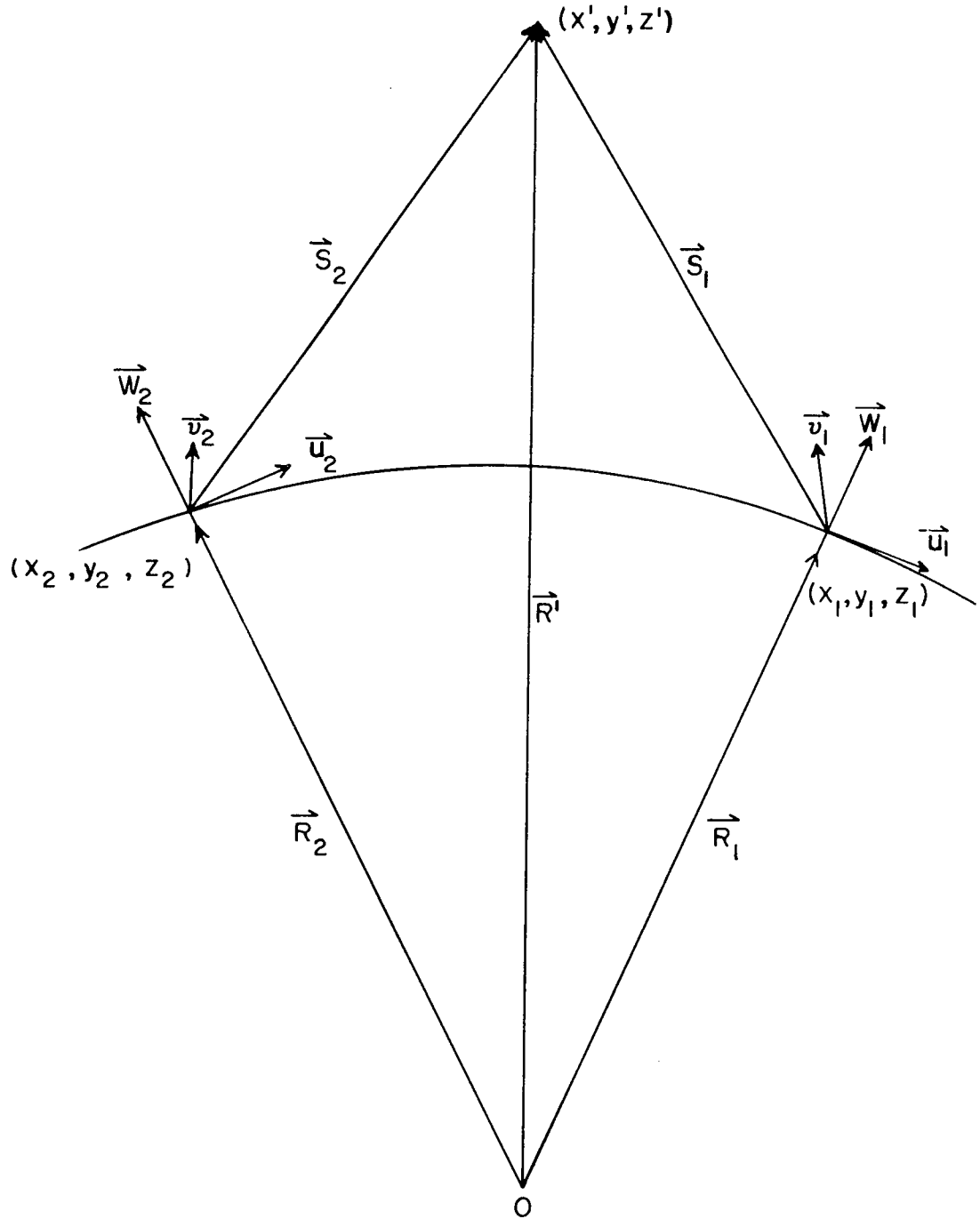


Figure 5 - Approximate Satellite Position

Similarly we have the expressions

$$y' = \frac{(z_2 - z_1) + \frac{a_{z1} y_1}{a_{y1}} - \frac{a_{z2} y_2}{a_{y2}}}{\frac{a_{z1}}{a_{y1}} - \frac{a_{z2}}{a_{y2}}} \quad (11)$$

$$z' = \frac{(x_2 - x_1) + \frac{a_{x1} z_1}{a_{z1}} - \frac{a_{x2} z_2}{a_{z2}}}{\frac{a_{x1}}{a_{z1}} - \frac{a_{x2}}{a_{z2}}} \quad (12)$$

Let the relation between the first and second order approximations be

$$\begin{aligned} x'' &= x' + \alpha \\ y'' &= y' + \beta \\ z'' &= z' + \gamma \end{aligned} \quad (13)$$

where x'' , y'' , z'' represent the second order approximations to satellite position and α , β , and γ are small corrective terms. Since our first approximation is fairly accurate, α , β , and γ will be small, and terms of the order of α^2 or less can be neglected. Hence, in the second order approximation, equation (5) becomes

$$\begin{aligned} R_{oi} &= \sqrt{(x' - x_T + \alpha)^2 + (y' - y_T + \beta)^2 + (z' - z_T + \gamma)^2} \\ &\quad + \sqrt{(x' - x_i + \alpha)^2 + (y' - y_i + \beta)^2 + (z' - z_i + \gamma)^2} \\ &\quad - C_i. \end{aligned} \quad (14)$$

Making a Maclaurin series expansion of $R_{oi}(\alpha, \beta, \gamma)$ about $\alpha = \beta = \gamma = 0$ and neglecting higher order terms of α , β , γ , i.e.

$$R_{0i} = R_{0i}(0,0,0) + \left[\frac{\partial R_{0i}}{\partial \alpha} \right]_{0,0,0} \alpha + \left[\frac{\partial R_{0i}}{\partial \beta} \right]_{0,0,0} \beta + \left[\frac{\partial R_{0i}}{\partial \gamma} \right]_{0,0,0} \gamma + \dots,$$

we obtain an expression of the form

$$R_{0i} = E_i \alpha + F_i \beta + G_i \gamma + D_i \quad (15)$$

where

$$E_i = \frac{x' - x_T}{T} + \frac{x' - x_i}{K_i},$$

$$F_i = \frac{y' - y_T}{T} + \frac{y' - y_i}{K_i},$$

$$G_i = \frac{z' - z_T}{T} + \frac{z' - z_i}{K_i},$$

$$D_i = T + K_i - C_i,$$

$$T = \sqrt{(x' - x_T)^2 + (y' - y_T)^2 + (z' - z_T)^2},$$

$$K_i = \sqrt{(x' - x_i)^2 + (y' - y_i)^2 + (z' - z_i)^2}.$$

Performing a similar procedure for equations (3) and (4) the following relations are obtained:

$$\cos \theta_i = J_i \alpha + N_i \beta + P_i \gamma + H_i \quad (16)$$

where

$$J_i = \frac{u_{ix}}{K_i} - \frac{L_i (x' - x_i)}{K_i^3},$$

$$N_i = \frac{u_{iy}}{K_i} - \frac{L_i (y' - y_i)}{K_i^3},$$

$$P_i = \frac{u_{iz}}{K_i} - \frac{L_i (z' - z_i)}{K_i^3},$$

$$H_i = \frac{L_i}{K_i},$$

$$L_i = u_{ix} (x' - x_i) + u_{iy} (y' - y_i) + u_{iz} (z' - z_i),$$

and $\cos \phi_i = S_i \alpha + U_i \beta + W_i \gamma + Q_i$ (17)

where

$$S_i = \frac{v_{ix}}{K_i} - \frac{M_i (x' - x_i)}{K_i^3},$$

$$U_i = \frac{v_{iy}}{K_i} - \frac{M_i (y' - y_i)}{K_i^3}$$

$$W_i = \frac{v_{iz}}{K_i} - \frac{M_i (z' - z_i)}{K_i^3}$$

$$Q_i = \frac{M_i}{K_i}$$

and $M_i = v_{ix} (x' - x_i) + v_{iy} (y' - y_i) + v_{iz} (z' - z_i)$. The coefficients of α , β , and γ , and the constants are determined quantities since x' , y' , and z' can be obtained from equations (10), (11), and (12) respectively.

Now the standard least squares technique is applied to equations (15), (16), and (17). This approach maximizes the combined probability associated with the measurements actually made of range, and the east-west and north-south direction cosines of two receiver stations. The probability is of the form $P = ke^{-\phi}$ and it is maximized by minimizing the exponent ϕ .⁴

This expression is of the form:

$$\begin{aligned}
\phi = & \frac{1}{2\sigma_1^2} (E_1 \alpha + F_1 \beta + G_1 \gamma + D_1 - R_{m1})^2 + \frac{1}{2\sigma_1^2} (E_2 \alpha \\
& + F_2 \beta + G_2 \gamma + D_2 - R_{m2})^2 + \frac{1}{2\sigma_2^2} (J_1 \alpha + N_1 \beta + P_1 \gamma \\
& + H_1 - \cos \theta_{m1})^2 + \frac{1}{2\sigma_2^2} (J_2 \alpha + N_2 \beta + P_2 \gamma + H_2 - \cos \theta_{m2})^2 \\
& + \frac{1}{2\sigma_3^2} (S_1 \alpha + U_1 \beta + W_1 \gamma + Q_1 - \cos \phi_{m1})^2 + \frac{1}{2\sigma_3^2} (S_2 \alpha + \\
& U_2 \beta + W_2 \gamma + Q_2 - \cos \phi_{m2})^2 , \tag{18}
\end{aligned}$$

where R_{m1} and R_{m2} are the measured values of range from stations 1 and 2, $\cos \theta_{m1}$ and $\cos \theta_{m2}$ are the measured values of east-west direction cosine, and $\cos \phi_{m1}$ and $\cos \phi_{m2}$ are the measured values of north-south direction cosine.

The standard deviation of measured range, σ_1^2 , reflects the accuracy with which range can be measured. The same is true for σ_2^2 and σ_3^2 , which represent the standard deviation of the east-west direction cosine and north-south direction cosine measurements respectively.

To minimize $\phi (\alpha, \beta, \gamma)$, the expressions

$$\frac{\partial \phi}{\partial \alpha} = 0,$$

$$\frac{\partial \phi}{\partial \beta} = 0,$$

$$\text{and} \quad \frac{\partial \phi}{\partial \gamma} = 0$$

are formed. By taking the derivative with respect to α , combining terms and setting the result equal to zero, we obtain

$$a_1 \alpha + b_1 \beta + c_1 \gamma = d_1 \quad (19)$$

where

$$a_1 = \frac{E_1^2 + E_2^2}{\sigma_1^2} + \frac{J_1^2 + J_2^2}{\sigma_2^2} + \frac{S_1^2 + S_2^2}{\sigma_3^2},$$

$$b_1 = \frac{E_1 F_1 + E_2 F_2}{\sigma_1^2} + \frac{J_1 N_1 + J_2 N_2}{\sigma_2^2} + \frac{S_1 U_1 + S_2 U_2}{\sigma_3^2},$$

$$c_1 = \frac{E_1 G_1 + E_2 G_2}{\sigma_1^2} + \frac{J_1 P_1 + J_2 P_2}{\sigma_2^2} + \frac{S_1 W_1 + S_2 W_2}{\sigma_3^2},$$

$$d_1 = - \left[\frac{E_1 (D_1 - R_{m1}) + E_2 (D_2 - R_{m2})}{\sigma_1^2} \right.$$

$$\left. + \frac{J_1 (H_1 - \cos \theta_{m1}) + J_2 (H_2 - \cos \theta_{m2})}{\sigma_2^2} + \frac{S_1 (Q_1 - \cos \phi_{m1}) + S_2 (Q_2 - \cos \phi_{m2})}{\sigma_3^2} \right].$$

By taking the derivative with respect to β , combining terms and setting the result equal to zero, we obtain

$$a_2 \alpha + b_2 \beta + c_2 \gamma = d_2, \quad (20)$$

where

$$a_2 = \frac{E_1 F_1 + E_2 F_2}{\sigma_1^2} + \frac{J_1 N_1 + J_2 N_2}{\sigma_2^2} + \frac{S_1 U_1 + S_2 U_2}{\sigma_3^2},$$

$$b_2 = \frac{F_1^2 + F_2^2}{\sigma_1^2} + \frac{N_1^2 + N_2^2}{\sigma_2^2} + \frac{U_1^2 + U_2^2}{\sigma_3^2} ,$$

$$c_2 = \frac{F_1 G_1 + F_2 G_2}{\sigma_1^2} + \frac{N_1 P_1 + N_2 P_2}{\sigma_2^2} + \frac{U_1 W_1 + U_2 W_2}{\sigma_3^2}$$

and

$$d_2 = - \left[\frac{F_1 (D_1 - R_{m1}) + F_2 (D_2 - R_{m2})}{\sigma_1^2} + \frac{N_1 (H_1 - \cos \theta_{m1}) + N_2 (H_2 - \cos \theta_{m2})}{\sigma_2^2} + \frac{U_1 (Q_1 - \cos \phi_{m1}) + U_2 (Q_2 - \cos \phi_{m2})}{\sigma_3^2} \right] .$$

Similarly by taking the derivative of ϕ with respect to γ , we obtain the expression

$$a_3 \alpha + b_3 \beta + c_3 \gamma = d_3, \quad (21)$$

where

$$a_3 = \frac{E_1 G_1 + E_2 G_2}{\sigma_1^2} + \frac{J_1 P_1 + J_2 P_2}{\sigma_2^2} + \frac{S_1 W_1 + S_2 W_2}{\sigma_3^2} ,$$

$$b_3 = \frac{F_1 G_1 + F_2 G_2}{\sigma_1^2} + \frac{N_1 P_1 + N_2 P_2}{\sigma_2^2} + \frac{U_1 W_1 + U_2 W_2}{\sigma_3^2} ,$$

$$c_3 = \frac{G_1^2 + G_2^2}{\sigma_1^2} + \frac{P_1^2 + P_2^2}{\sigma_2^2} + \frac{W_1^2 + W_2^2}{\sigma_3^2} ,$$

and

$$d_3 = - \left[\frac{G_1 (D_1 - R_{m1}) + G_2 (D_2 - R_{m2})}{\sigma_1^2} \right]$$

$$+ \left[\frac{P_1(H_1 - \cos \theta_{m1}) + P_2(H_2 - \cos \theta_{m2})}{\sigma_2^2} + \frac{W_1(Q_1 - \cos \phi_{m1}) + W_2(Q_2 - \cos \phi_{m2})}{\sigma_3^2} \right].$$

By solving equations (19), (20), and (21) simultaneously, the values of α , β , and γ can be obtained which make ϕ in eq. (18) a minimum:

$$\alpha = \frac{\sum_{ijk} \epsilon_{ijk} d_i b_j c_k}{\sum_{ijk} \epsilon_{ijk} a_i b_j c_k}$$

$$\beta = \frac{\sum_{ijk} \epsilon_{ijk} a_i d_j c_k}{\sum_{ijk} \epsilon_{ijk} a_i b_j c_k}$$

$$\gamma = \frac{\sum_{ijk} \epsilon_{ijk} a_i b_j d_k}{\sum_{ijk} \epsilon_{ijk} a_i b_j c_k} .$$

The second order approximation to satellite position can now be obtained from equations (13).

At this point a check is made to see whether or not α , β , and γ are all within a specified tolerance. If they are not, the approximate position coordinates obtained in equations (10), (11), and (12) are replaced by the coordinates obtained in equations (13), i.e., (x'' , y'' , z''). Then the expansion and the least squares fit are repeated producing a new set of corrective terms. This iterative process is repeated until all of the corrective terms (α , β , and γ) are within the specified tolerance.

Velocity Determination

From a single satellite pass at a given receiver stations three parameters are measured which can be used to determine the velocity of

the satellite. These are east-west and north-south phase rate and the doppler frequency shift. These measurements are discussed in Chapter I.

This information received from each of two receiver stations results in six input parameters from which the three velocity components are to be computed. The coordinate system to be used is the same as that discussed in Chapter I.

An expression relating doppler shift and velocity components can be obtained as follows:

$$\frac{dR_{oi}}{dt} = \frac{\partial R_{oi}}{\partial x} \frac{dx}{dt} + \frac{\partial R_{oi}}{\partial y} \frac{dy}{dt} + \frac{\partial R_{oi}}{\partial z} \frac{dz}{dt} ,$$

where R_{oi} is the bistatic range and is defined in eq. (5), or

$$\begin{aligned} \frac{dR_{oi}}{dt} = & \left[\frac{(x - x_T)}{\sqrt{(x - x_T)^2 + (y - y_T)^2 + (z - z_T)^2}} + \frac{(x - x_i)}{\sqrt{(x - x_i)^2 + (y - y_i)^2 + (z - z_i)^2}} \right] \frac{dx}{dt} \\ & + \left[\frac{(y - y_T)}{\sqrt{(x - x_T)^2 + (y - y_T)^2 + (z - z_T)^2}} + \frac{(y - y_i)}{\sqrt{(x - x_i)^2 + (y - y_i)^2 + (z - z_i)^2}} \right] \frac{dy}{dt} \\ & + \left[\frac{(z - z_T)}{\sqrt{(x - x_T)^2 + (y - y_T)^2 + (z - z_T)^2}} + \frac{(z - z_i)}{\sqrt{(x - x_i)^2 + (y - y_i)^2 + (z - z_i)^2}} \right] \frac{dz}{dt} . \end{aligned}$$

Inserting the optimum position coordinates into the above expressions for T and K_i , the above equation can be written

$$\begin{aligned} \frac{d R_{oi}}{dt} = & \left[\frac{x - x_T}{T} + \frac{x - x_i}{K_i} \right] \frac{dx}{dt} + \left[\frac{y - y_T}{T} + \frac{y - y_i}{K_i} \right] \frac{dy}{dt} \\ & + \left[\frac{z - z_T}{T} + \frac{z - z_i}{K_i} \right] \frac{dz}{dt} . \end{aligned}$$

$$\text{Now } D_{oi} = - \frac{f}{c} \frac{d R_{oi}}{dt}$$

where D_{oi} is the calculated doppler frequency shift, f is the frequency of the transmitted signal, and c is the velocity of light. Therefore we have

$$\begin{aligned} D_{oi} = & \left(- \frac{f}{c} \right) \left[\frac{x - x_T}{T} + \frac{x - x_i}{K_i} \right] \frac{dx}{dt} + \left(- \frac{f}{c} \right) \left[\frac{y - y_T}{T} + \frac{y - y_i}{K_i} \right] \frac{dy}{dt} \\ & + \left(- \frac{f}{c} \right) \left[\frac{z - z_T}{T} + \frac{z - z_i}{K_i} \right] \frac{dz}{dt} . \end{aligned} \quad (22)$$

A relationship between east-west rate and the velocity components can be obtained from the relationship

$$\frac{d}{dt} (\cos \theta_i) = \frac{\partial}{\partial x} (\cos \theta_i) \frac{dx}{dt} + \frac{\partial}{\partial y} (\cos \theta_i) \frac{dy}{dt} + \frac{\partial}{\partial z} (\cos \theta_i) \frac{dz}{dt} .$$

Using eq. (3) and inserting the optimum position coordinates into the above expressions for L_i and M_i we obtain

$$\begin{aligned} \frac{d}{dt} (\cos \theta_i) = & \left[\frac{K_i u_{ix} - L_i (x - x_i)}{K_i^2} \right] \frac{dx}{dt} \\ & + \left[\frac{K_i u_{iy} - L_i (y - y_i)}{K_i^2} \right] \frac{dy}{dt} \end{aligned}$$

$$+ \left[\frac{K_i u_{iz} - \frac{L_i (z - z_i)}{K_i}}{K_i^2} \right] \frac{dz}{dt} ,$$

or

$$\begin{aligned} \frac{d}{dt} (\cos \theta_i) = & \left[\frac{u_{ix}}{K_i} - \frac{L_i (x - x_i)}{K_i^3} \right] \frac{dx}{dt} + \left[\frac{u_{iy}}{K_i} - \frac{L_i (y - y_i)}{K_i^3} \right] \frac{dy}{dt} \\ & + \left[\frac{u_{iz}}{K_i} - \frac{L_i (z - z_i)}{K_i^3} \right] \frac{dz}{dt} . \end{aligned} \quad (23)$$

The expression relating north-south rate and velocity components can be derived in a manner similar to eq. (23) and is

$$\begin{aligned} \frac{d}{dt} (\cos \phi_i) = & \left[\frac{v_{ix}}{K_i} - \frac{M_i (x - x_i)}{K_i^3} \right] \frac{dx}{dt} \\ & + \left[\frac{v_{iy}}{K_i} - \frac{M_i (y - y_i)}{K_i^3} \right] \frac{dy}{dt} + \left[\frac{v_{iz}}{K_i} - \frac{M_i (z - z_i)}{K_i^3} \right] \frac{dz}{dt} . \end{aligned} \quad (24)$$

Using the results of the position determination section for x , y , and z , the coefficients of equations (22), (23), and (24) can be determined. Hence, we have six linear equations containing three unknowns. These equations can be combined in a least squares sense to determine the values of velocity components best fitting the data.

The ϕ equation can be formed as was done above, in the determination of optimum position coordinates. Then the expressions

$$\frac{\partial \phi}{\partial v_x} = 0,$$

$$\frac{\partial \phi}{\partial v_y} = 0,$$

$$\frac{\partial \phi}{\partial v_z} = 0,$$

where

$$v_x = \frac{dx}{dt},$$

$$v_y = \frac{dy}{dt},$$

and

$$v_z = \frac{dz}{dt}$$

can be formed to yield three linear equations in three unknowns. The values of v_x , v_y , and v_z can then be determined which best fit the data.

In the velocity development no expansion is necessary since equations (22), (23), and (24) are linear.

Determination of Classical Elements

At this point in the development we have determined the position and velocity of the satellite in an earth-fixed coordinate set (\vec{R} and $\dot{\vec{R}}$). By a series of transformations these six elements can be reduced to the six classical elliptical elements: inclination (i), semi-major axis (a), eccentricity (e), argument of perigee (ω), right ascension of the ascending node (Ω), and true anomaly (ν). These elements are defined in the

literature⁵. Eccentricity is dimensionless, a is measured in statute miles, and the remaining four elements are measured in degrees. The elements are given for an instant in time which is called epoch time. In this thesis the epoch time will be the time of the satellite observation.

The orbit model chosen considers only the first order secular perturbations, the motion of the node, $\dot{\Omega}$, and the motion of perigee, $\dot{\omega}$.⁶

First a transformation is made from the earth fixed system to one in which the orbit plane is fixed (x', y', z'). This transformation is discussed in Appendix A. In this system inclination and right ascension can be computed. Inclination is computed by finding the angle between the normals to the orbital and equatorial planes:

$$i = \cos^{-1} \left[\vec{k} \cdot \frac{\vec{R}' \times \dot{\vec{R}}'}{|\vec{R}' \times \dot{\vec{R}}'|} \right].$$

Before right ascension can be computed the position of the node must be found. The west longitude of the ascending node (λ_N) is obtained by first forming a vector ($\vec{\alpha}$) along the line of nodes pointing towards the ascending node:

$$\vec{\alpha} = \vec{k} \times \frac{\vec{R}' \times \dot{\vec{R}}'}{|\vec{R}' \times \dot{\vec{R}}'|}.$$

The direction of $\vec{R}' \times \dot{\vec{R}}'$ is normal to the orbital plane; hence $\vec{\alpha}$ must be both in the orbital plane and in the x, y plane (normal to \vec{k}). But the intersection of these two planes is the line of nodes; hence $\vec{\alpha}$ lies along the line of nodes. The angle (less than 180°) formed by the x -axis (0° longitude) and $\vec{\alpha}$ is obtained from the expression

$$\lambda = \cos^{-1} \left[\frac{\vec{i} \cdot \vec{\alpha}}{|\vec{\alpha}|} \right],$$

and from this angle the longitude of the ascending node can be computed. The right ascension of the ascending node can then be obtained from the longitude of the node and the west longitude (Greenwich Hour Angle) of the first point of Aries at epoch time. These angles are illustrated in Figure 6, where γ is the first point of Aries.

At this point in the development, a series of transformations are made transforming the position and velocity vectors from the coordinate set in which the orbit plane is fixed (x' , y' , z') to one which the ellipse is fixed and lies in the x , y plane (\vec{R} , $\dot{\vec{R}}$). These transformations are discussed in Appendix A.

The purpose of all the transformations discussed in this chapter and in appendix A is to transform out the perturbations due to the oblateness terms in the earth's potential and to reduce the problem to the undisturbed two-body one.

The law of conservation of energy yields the formula ^{7,8}

$$\dot{\vec{R}}^2 = \gamma (M + m) \left[\frac{2}{R} - \frac{1}{a} \right] \quad (25)$$

where γ is the gravitational constant, M is the mass of the earth, m is the mass of the satellite, and $\dot{\vec{R}}$ and \vec{R} are the magnitudes of $\dot{\vec{R}}$ and \vec{R} respectively. We can neglect m since $M \gg m$ and, upon solving for a , equation (25) becomes

$$a = \frac{-1}{\frac{\dot{\vec{R}}^2}{\gamma M} - \frac{2}{R}}$$

or

$$a = - \frac{\gamma M}{\frac{\dot{\vec{R}}^2}{R} - \frac{2\gamma M}{R}} \quad (26)$$

Since γM is a known constant, the semi-major axis of the orbit is therefore determined. The area integral for the two body problem is^{9,10}

$$\vec{R} \times \frac{d\vec{R}}{dt} = \vec{h}, \quad (27)$$

where \vec{h} is a constant vector, normal to the orbit plane, having magnitude

$$h = \sqrt{\gamma (M + m) a (1 - e^2)}. \quad (28)$$

From eqs. (27) and (28), it follows that

$$\left| \vec{R} \times \dot{\vec{R}} \right|^2 = \gamma M a (1 - e^2)$$

or

$$e = \sqrt{1 - \frac{\left| \vec{R} \times \dot{\vec{R}} \right|^2}{\gamma M a}}, \quad (29)$$

where again m is neglected and a is obtained from equation (26). Eq.

(29) gives us an expression for the eccentricity of the orbit.

Once a and e have been determined, it is then possible to compute true anomaly (v) using the equation of a conic section in polar coordinates:

$$r = \frac{p}{1 + e \cos v}.$$

For an ellipse¹¹

$$p = a(1 - e^2).$$

Hence we have, in the $(\bar{x}, \bar{y}, \bar{z})$ reference frame,

$$\bar{R} = \frac{a(1 - e^2)}{1 + e \cos v}.$$

Solving for v we obtain

$$v = \cos^{-1} \left[\frac{a(1 - e^2)}{\bar{R} e} - \frac{1}{e} \right],$$

where
$$0 \leq v \leq \pi \text{ if } \vec{R} \cdot \dot{\vec{R}} > 0$$

and
$$\pi \leq v \leq 2\pi \text{ if } \vec{R} \cdot \dot{\vec{R}} < 0.$$

From the definitions of the classical elements, it can be seen that the angle (β) along the orbit, from the ascending node to the satellite equals the sum of anomaly and argument of perigee. Figure 7 shows angle β along with the satellite position in the \bar{x}, \bar{y} plane. Now the nature of the transformations is such that β increases in a counterclockwise sense. Hence if \bar{y} is positive or zero, $0 \leq \beta \leq \pi$ and

$$\beta = \cos^{-1} \left[\frac{\bar{x}}{\bar{R}} \right]$$

and if \bar{y} is negative, $\pi < \beta < 2\pi$ and

$$\beta = 2\pi - \cos^{-1} \left[\frac{\bar{x}}{\bar{R}} \right].$$

In either case the argument of perigee is computed from

$$\omega = \beta - v.$$

The computational scheme is as follows. First the transformation is made that fixes the orbit plane in space. A value of $\dot{\Omega}$ must be assumed since no elements have been computed. Then inclination and the longitude of the ascending node are computed in this system. With the assumptions that $e = 0$ and $a =$ radius of the earth, $\dot{\omega}$ is calculated and the rest of the transformations discussed in Appendix A are made, fixing the ellipse in the x, y plane.

In this system $(\bar{x}, \bar{y}, \bar{z})$, a , e , and v are computed, and the values of i , a and e are used to calculate new values of $\dot{\omega}$ and $\dot{\Omega}$. All of the transformations are repeated using the new $\dot{\omega}$ and $\dot{\Omega}$ values, and i , λ_N , a , e , and v are recalculated. At this point a check is made to see if both the eccentricity and the anomaly of two successive iterations are within a

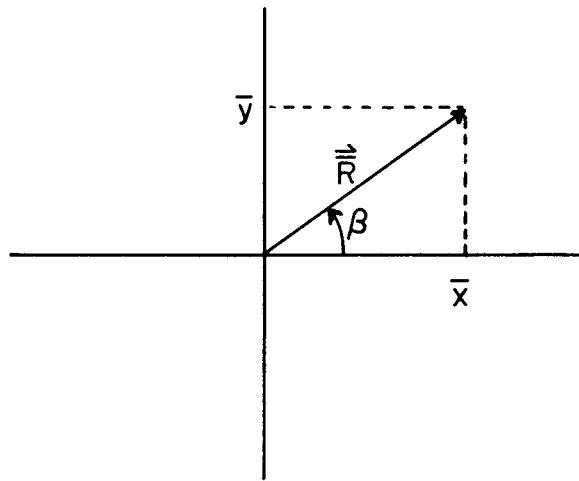


Figure 7 - Sum of Anomaly and Argument of Perigee in \bar{X} , \bar{Y} Plane

specified tolerance. The process is repeated until both tolerances are satisfied, at which time the argument of perigee and right ascension are computed from the results of the last iteration and the problem is solved.

CHAPTER III

ERROR ANALYSIS

Method of Error Determination

Errors existing in the measured parameters will produce corresponding errors in the orbital elements derived from these measurements. Once the elements have been obtained, the corresponding path of the satellite can be computed. The true path of the satellite can be obtained in a similar manner by starting with parameters which contain no errors. The errors in the measured parameters can then be analyzed by studying the resulting deviation of the satellite's path from its true path. This, in general, is the method used for the error analyses in this development. It was used for two purposes: to determine experimentally the advantages of using all available input in the computation of "single-pass" elements, and to study theoretically the degree of error reduction caused by the addition of certain parameters.

The input of the method consists of two sets of orbital elements. The first set is the reference set. It has no errors associated with it and is called the unperturbed set. The second set has errors associated with it and is called the perturbed set. In Figure 8 at time t_0 the unperturbed satellite is at P_0 and the perturbed satellite is at P_0' . These positions are calculated directly from the elements and are in the earth fixed coordinate system discussed in Chapter I. The anomaly of the unperturbed orbit is then increased by a specified amount, moving the unperturbed satellite to P_1 . The time $(t_1 - t_0)$ required for this anomaly change is then computed and the unperturbed elements are updated

to time t_1 . The coordinates of P_1 are then computed from the updated elements and an error plane normal to the unperturbed orbit plane at P_1 , and passing through the center of the earth, is set up. In this plane \vec{R} is a unit vector pointing in the direction of the radius vector to point P_1 , and \vec{A} is a unit vector normal to the plane of the reference orbit. Now in a similar fashion the anomaly of the perturbed orbit is increased by the above increment, moving the perturbed satellite to P_2 . The point P_3 , which is the intersection of the perturbed orbit with the error plane is then obtained. At this point three errors are computed; the time error in seconds, which is the time that the perturbed satellite passes through the error plane minus the time that the unperturbed satellite passes through the error plane (Δt), the height error along \vec{R} (Δh), and the cross-track error along \vec{A} (Δx), both in statute miles. The mathematical expressions for these errors are given below. The unperturbed anomaly is again advanced and the process is repeated, again producing three errors. This process is repeated for as many anomaly increments as desired. At each point the unperturbed central angle from P_0 to the error plane is computed, e.g. θ in Figure 8, and a plot is made of error versus central angle.

The computation of the vectors \vec{R} and \vec{A} , for example at t_1 , is as follows. Let \vec{R}_1 be the position vector to P_1 ; then, since we have obtained x_1 , y_1 , and z_1 , we can compute \vec{R} from

$$\vec{R} = \frac{\vec{R}_1}{|\vec{R}_1|} .$$

Since the unperturbed elements are updated to time t_1 , we know the longitude of the ascending node (λ_N) at this time and we can construct a

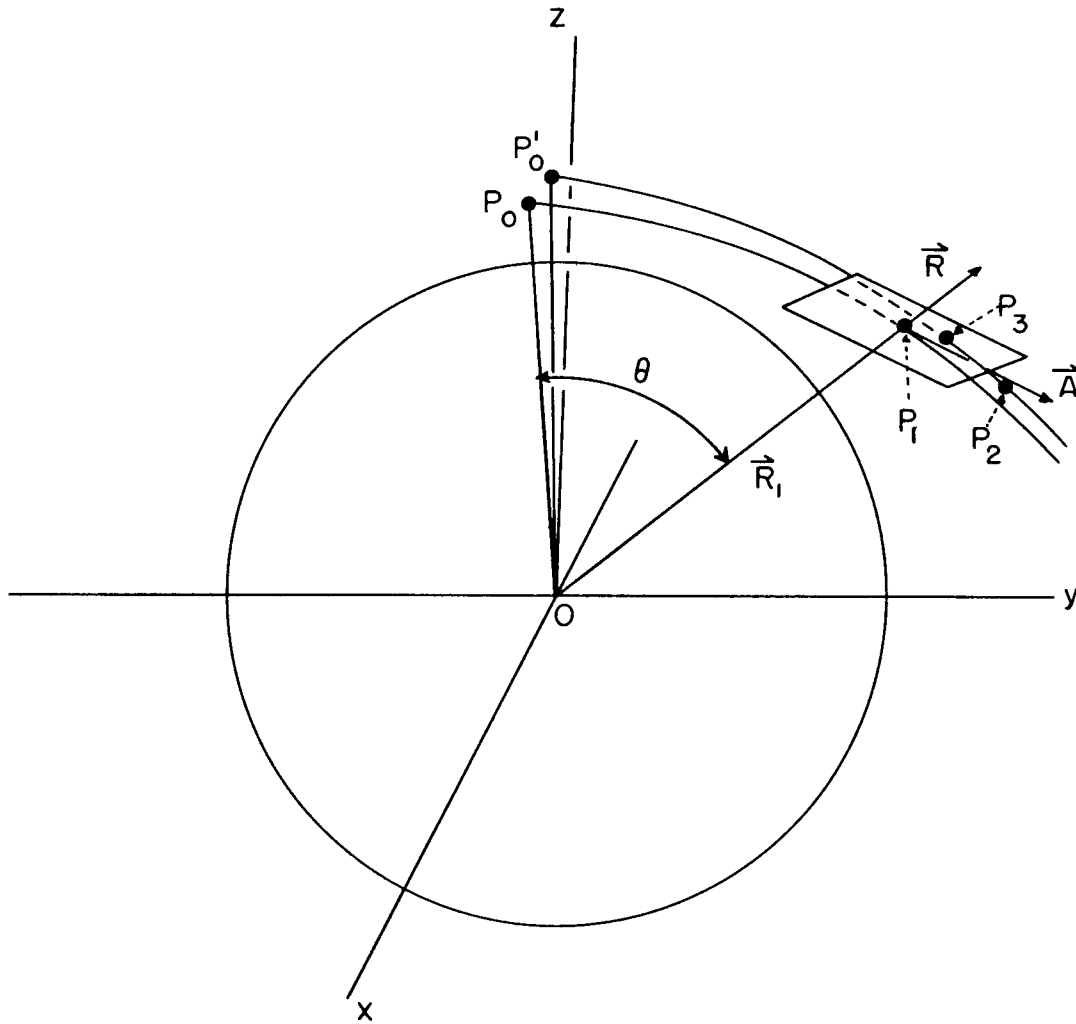


Figure 8 - Representation of Error Plane at Central Angle θ

vector \vec{B} lying along the line of nodes and pointing towards the ascending node:

$$\vec{B} = \vec{i} \cos \lambda_N - \vec{j} \sin \lambda_N.$$

We can therefore obtain a unit vector normal to the orbit plane from the expression

$$\vec{A} = \frac{\vec{B} \times \vec{R}_1}{|\vec{B} \times \vec{R}_1|}.$$

The unit vector normal to the error plane is given by

$$\vec{N} = \vec{A} \times \vec{R}.$$

The normal distance from P_2 to the error plane is given by

$$d = \vec{N} \cdot (\vec{P}_2 - \vec{P}_1) \quad (30)$$

(see Fig. 9), and the approximate correction of central angle to find point P_3 is

$$\Delta\theta = \frac{\vec{N} \cdot (\vec{P}_2 - \vec{P}_1)}{|\vec{R}_2|} \quad (31)$$

where \vec{R}_2 is the vector from the center of the earth to point P_2 .

From $\Delta\theta$ the perturbed elements can be corrected and an approximation to point P_3 (P_3') can be computed. In equation (30) P_2 is replaced by P_3' and d is again computed. If d is less than a specified tolerance, P_3' is used as the intersection of the perturbed orbit with the error plane (i.e. $P_3' = P_3$). If d is not within the tolerance, the central angle correction is repeated [eq. (31)] using P_3' and \vec{R}_3' in place of P_2 and \vec{R}_2 , and this is used to produce a second approximation to P_3 (i.e. P_3'').

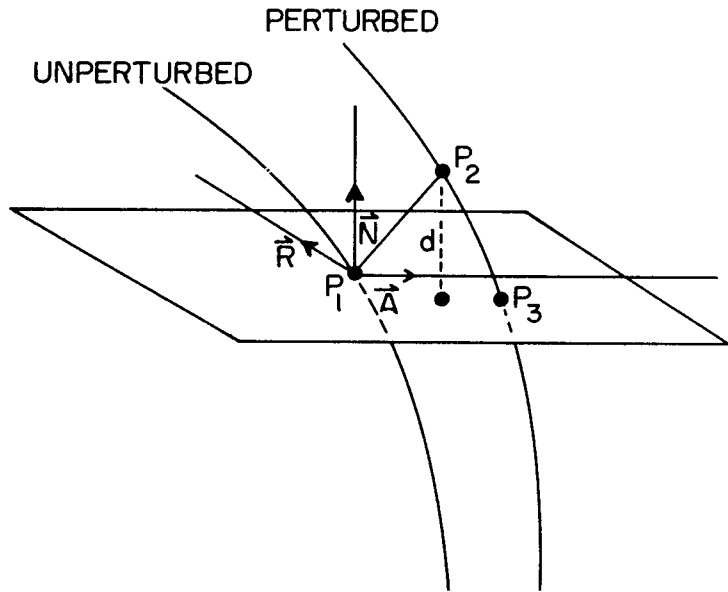


Figure 9 - Distance from P_2 to the Error Plane

This iterative process is repeated until d is within the tolerance. Once the coordinates of P_3 are found the errors in the error plane are computed from the following formulae [Fig. 10]:

$$\Delta x = \vec{A} \cdot (\vec{P}_3 - \vec{P}_1),$$

and

$$\Delta h = \vec{R} \cdot (\vec{P}_3 - \vec{P}_1).$$

The error out of the error plane (Δt) is expressed in seconds and is the time required for the satellite to go from P_3 to P_2 . If desired, the distance between the points P_1 and P_3 can be computed from the expression

$$\Delta R = \sqrt{(\Delta x)^2 + (\Delta h)^2}$$

and ΔR can be plotted versus central angle.

This method of error analysis was devised and adapted for use on the NAREC electronic computer by the author and James A Buisson III under the supervision of Donald W. Lynch.

Dependence of Errors on Accuracy of Measured Doppler Shift

We will now discuss the analytical method of studying system accuracy. This method makes use of the above mentioned method of error analysis. First a nominal set of orbital elements is selected. In this analysis a one-thousand-mile-high circular orbit, inclined at 50° with the equator, was used. This orbit is then employed together with a prediction scheme to predict a "fence" crossing. This prediction program gives the time of fence crossing together with satellite direction, east-west and north-south angles and direction cosine rates, range, and doppler shift. This information is used as input to the scheme discussed in Chapter II to produce the unperturbed (reference) orbit. This is actually nothing more than the above mentioned nominal set of

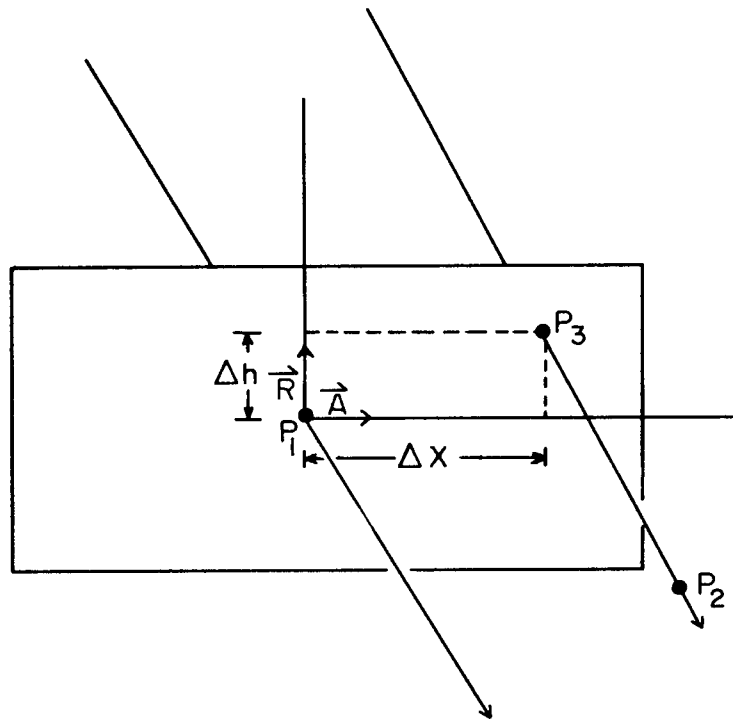


Figure 10 - Representation of Errors Δx and Δh

elements updated to the time of "fence" crossing. Then one of the input parameters is varied by an amount equivalent to the errors involved in the measurement of that parameter. The rest of the parameters are not changed and are used with this varied parameter to produce the perturbed orbit. The unperturbed and perturbed orbits are then used in the error scheme discussed above to generate Δx , Δh , and Δt error curves. This gives us a measure of the effect that the accuracy of a measured parameter has on the resulting orbital elements. If the effect of more than one parameter is desired, errors are computed for each parameter as described above, and are combined by summing the squares of the individual errors and taking the square root. This is done for each value of central angle, and the errors are called Δx_{RSS} , Δh_{RSS} , and Δt_{RSS} . For example we have for Δx_{RSS}

$$\Delta x_{RSS} = \sqrt{(\Delta x_1)^2 + (\Delta x_2)^2 + \dots + (\Delta x_N)^2} .$$

The error ΔR_{RSS} appears in the curves below. The defining equation for this error is

$$\Delta R_{RSS} = \sqrt{(\Delta x_{RSS})^2 + (\Delta h_{RSS})^2} .$$

The following is an example of how the addition of doppler shift measurement reduces Δx_{RSS} , Δh_{RSS} , Δt_{RSS} , and ΔR_{RSS} when measurements are made on a satellite having the above mentioned nominal orbital elements. Since range is not part of the present system, it was eliminated by making the standard deviation (σ_1) associated with its measurement a very large number (10^{20} miles). This has the effect of making the terms associated with range in equation (18) negligible compared with the other terms. The errors Δx_{RSS} , Δh_{RSS} , Δt_{RSS} , and ΔR_{RSS} are computed by individually perturbing east-west angle, north-south angle, doppler shift, rate of

change of east-west direction cosine, and rate of change of north-south direction cosine from both receiving stations. All parameters are perturbed by their corresponding sigma values. These errors are produced for several values of doppler shift standard deviation (i.e. $\sigma_D = 10, 10^2, 10^3, 10^4, 10^5, 10^{20}$). For each case, a set of error curves is obtained and the dependence of a given error (e.g. Δx_{RSS}) on σ_D for this particular case can be studied. In Figure 11, the Δx_{RSS} curves for the six above values of σ_D are plotted. Similarly in Figures 12, 13, and 14 the Δh_{RSS} , Δt_{RSS} , and ΔR_{RSS} error curves, respectively, are plotted for the six values of σ_D . In the figures, curves A, B, C, D, E, and F refer to errors computed with $\sigma_D = 10, 10^2, 10^3, 10^4, 10^5$, and 10^{20} respectively, and curve T is a plot of time after epoch versus central angle. In the figures the central angle varies from 0° to 360° and the errors vary from 0 to 1. To normalize the errors, Δx_{RSS} values were divided by 100, and Δh_{RSS} , Δt_{RSS} , and ΔR_{RSS} values were divided by 1000. Also, for normalization purposes, the values of time used in the T curves were divided by 100. It should be pointed out that these error curves apply only to the nominal orbit mentioned above and to satellites whose orbital elements are very similar to these nominal elements. General conclusions concerning the effect of doppler shift on the reduction of errors in any satellite orbit cannot be drawn until the individual results of a large cross section of different nominal sets are studied.

In Figure 11 curves C, D, E, and F are identical. Curve F ($\sigma_D = 10^{20}$) corresponds to errors that exist when doppler shift is not used. Therefore in this case, for doppler shift to produce a reduction in cross track error (Δx), it must be measured to an accuracy of better

than 1000 cps. In the case of cross track error, the most significant error reduction occurs for values of central angle of 90° and 270° . And the reduction of σ_D from 100 to 10 cps produces the most pronounced error reduction at these values of central angle.

In Figure 12 the most significant reduction in height error (Δh_{RSS}) occurs when σ_D is reduced from 10^3 to 10^2 , and the values of central angle at which the addition of doppler shift measurement produces the largest error reduction are 60° and 280° .

In Figure 13, even for accurately measured doppler shift, the time error (Δt_{RSS}) curves are not symmetrical and for values of central angle greater than 180° the errors are considerably larger than for small central angle. The time error in seconds is the same order of magnitude as the height error in miles. But since the velocity of the satellite is approximately 5 miles per second, the time error represents an error in distance which is larger than Δh . Therefore, in the case of our nominal set, it can be seen from Figure 13 that, in the first revolution after observation, the addition of accurately measured doppler results in an improvement mainly in the first 180° of central angle. In this region the largest error reduction occurs at a central angle of 130° . The most significant reduction in time error in this case occurs when σ_D is reduced from 10^3 to 10^2 cps.

The curve of ΔR_{RSS} vs. θ in Figure 14 is very similar to the Δh_{RSS} vs. θ curves (Figure 12), and everything said above concerning Figure 12 applies also to Figure 14.

Dependence of Errors on Accuracy of Measured Range

The above error analysis was also run for several values of standard deviation associated with measured range (σ_1). The values of σ_1 used

were 0.1, 1.0, 10.0, and 10^{20} miles. The errors Δx_{RSS} , Δh_{RSS} , Δt_{RSS} , and ΔR_{RSS} are again computed by individually perturbing east-west angle, north-south angle, doppler shift, rate of change of east-west direction cosine, and rate of change of north-south direction cosine from both receiver stations. All parameters are again perturbed by their operational sigma values with a σ of 10.0 cps being assumed for doppler shift. For each value of σ_1 , error curves are generated and, for the nominal orbit chosen, the dependence of R.S.S. errors on σ_1 is obtained.

It was found that the error curves were the same for each value of σ_1 and were identical to curves A in figures 11, 12, 13, and 14. Since the curves generated for $\sigma_1 = 10^{20}$ represent the errors in the system when range is not included it was concluded, for the particular case chosen, that the addition of a range measurement, even to the accuracy of 0.1 miles, resulted in no appreciable reduction of error. This results from the fact that the errors in the parameters measuring the initial velocity components (i.e. doppler shift and phase-rate) produce errors in subsequent predicted positions of the satellite which are much larger than the errors in predicted satellite position owing to errors in the parameters measuring the initial position components (i.e. direction cosine). Hence, even though the introduction of a range measurement reduces the error in the initial position of the satellite, the errors in subsequent positions of the satellite are essentially not affected.

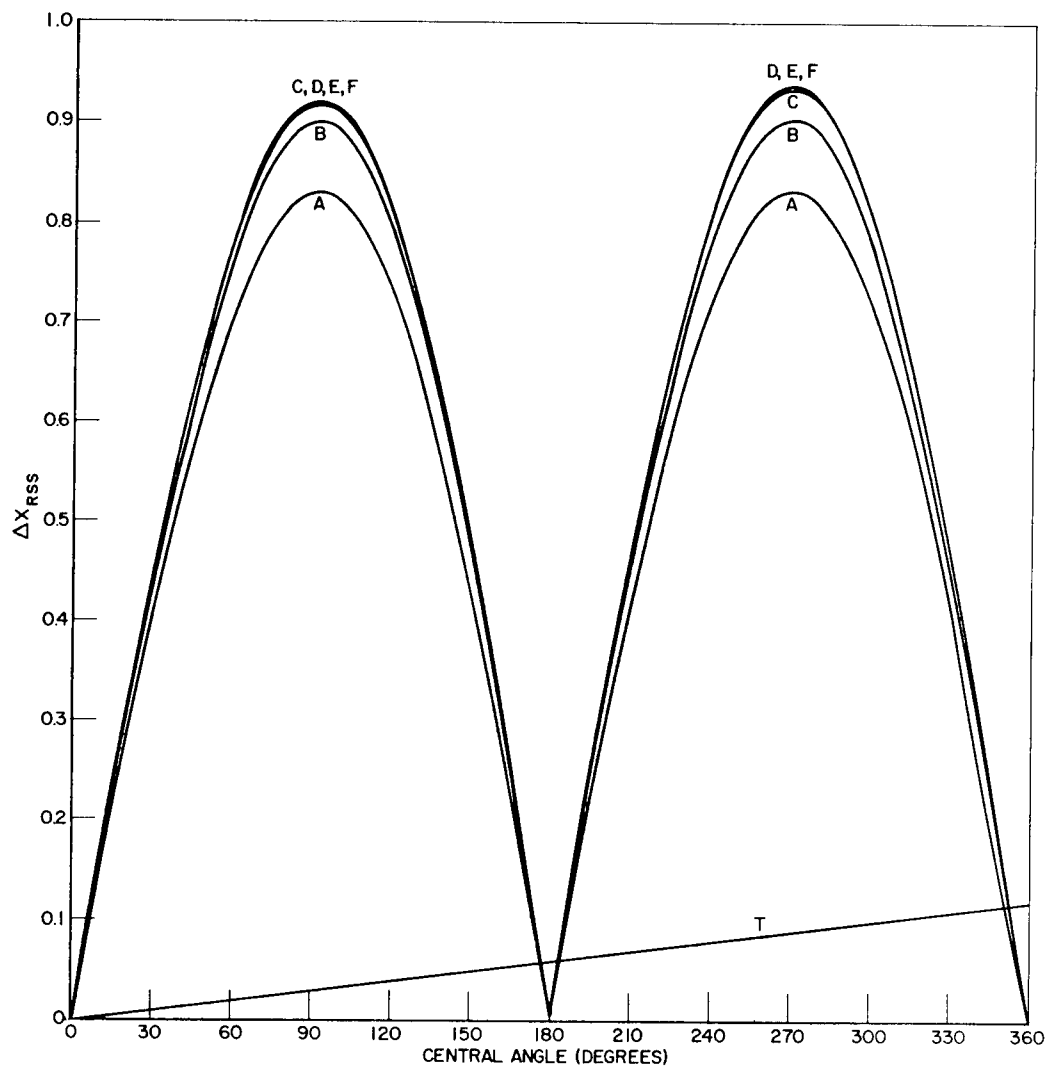


Figure 11 - Relation Between R.S.S. Cross Track Error and Central Angle

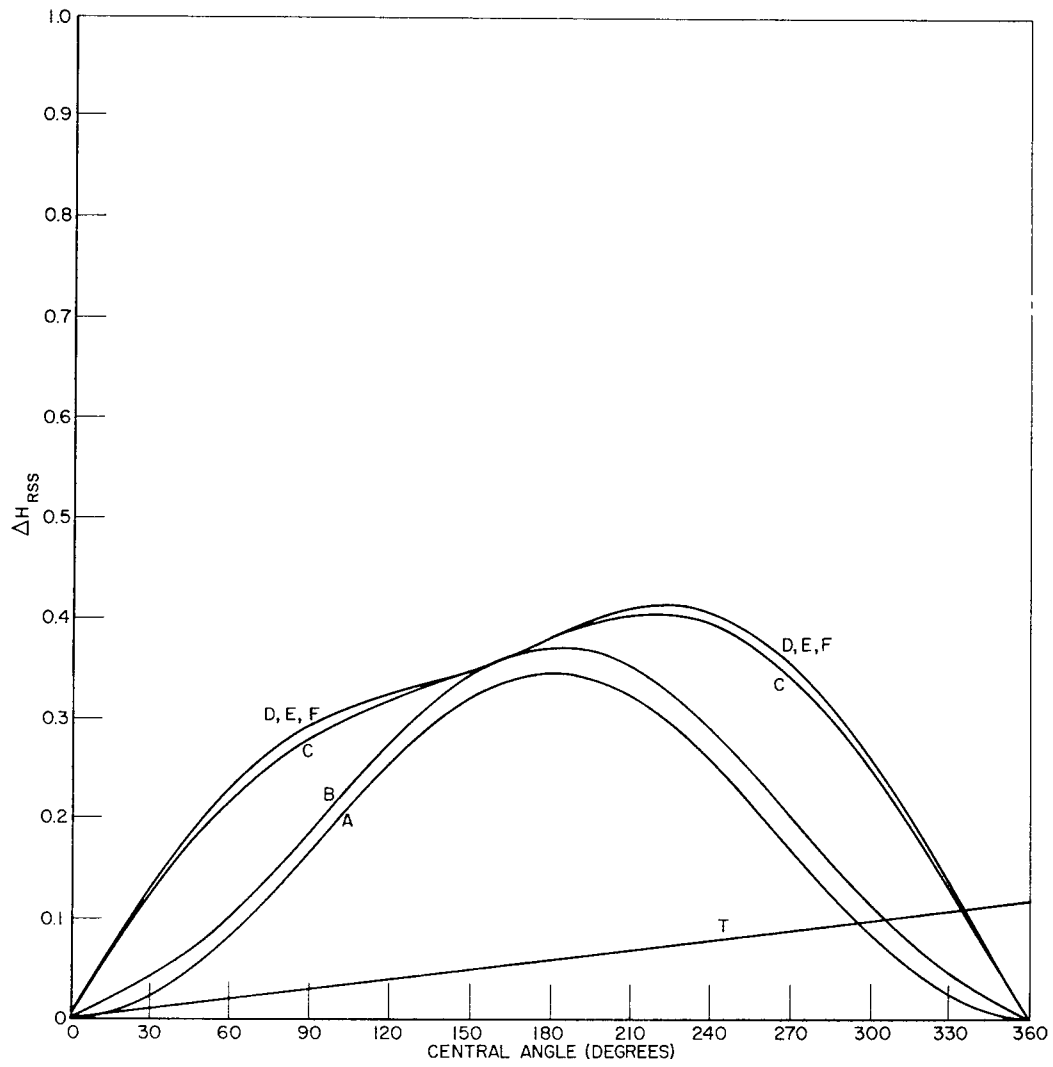


Figure 12 - Relation Between R.S.S. Height Error and Central Angle

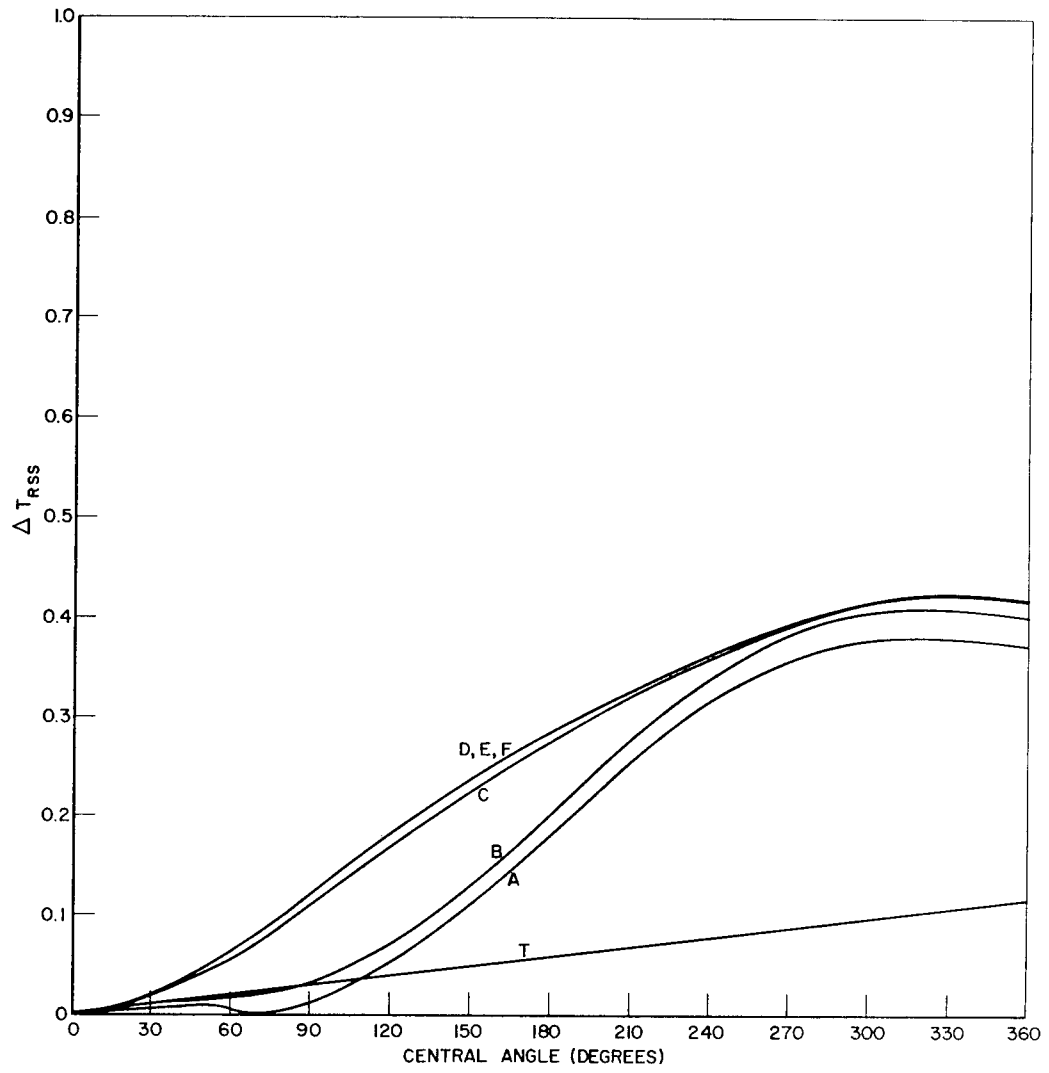


Figure 13 - Relation Between R.S.S. Time Error and Central Angle

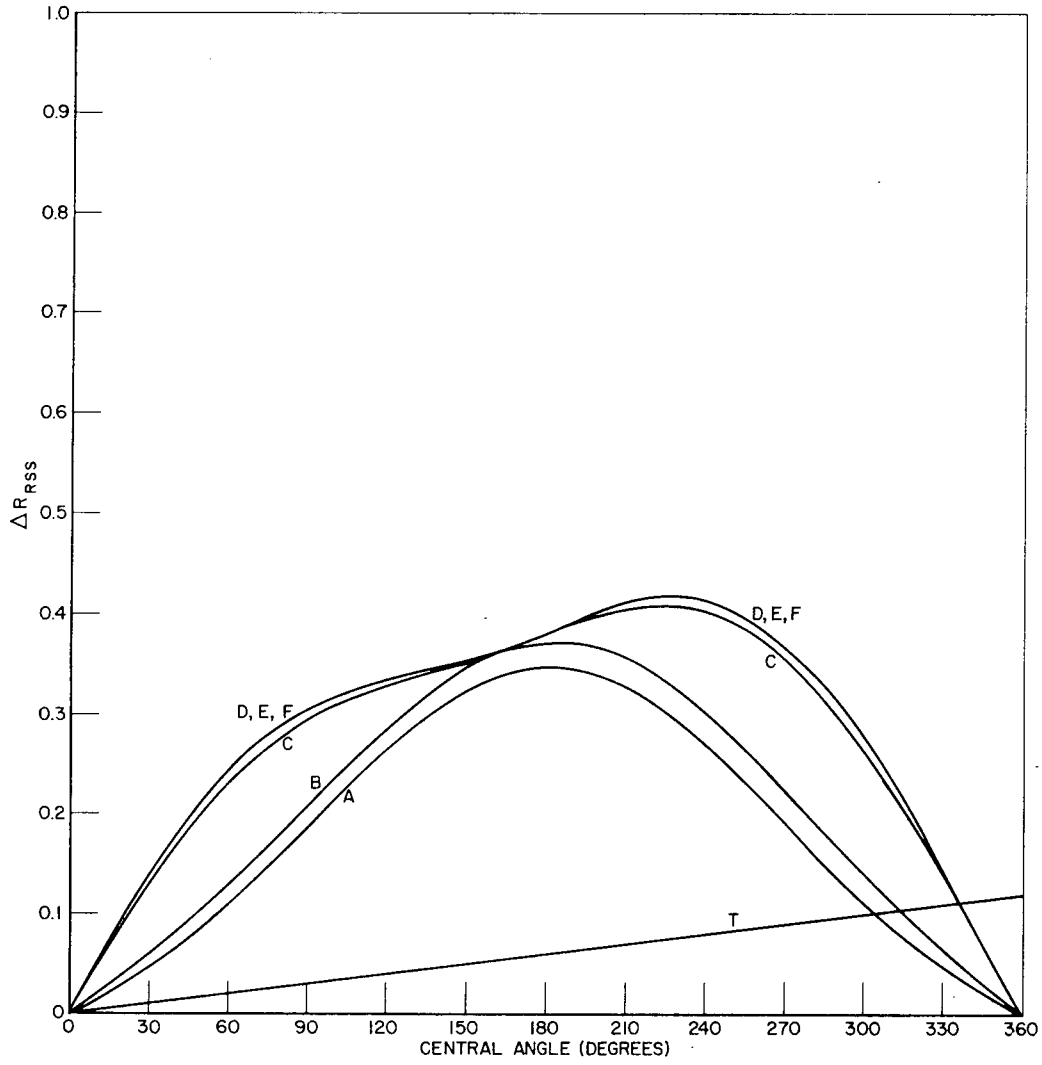


Figure 14 - Relation Between ΔR_{RSS} and Central Angle

CHAPTER IV

EXPERIMENTAL RESULTS

Equipment was installed at the Fort Stewart, Georgia, and Silver Lake, Mississippi, Space Surveillance receiving stations to measure doppler shift. The satellite used in this study was Echo I. Measurements were taken for approximately 200 separate passes of this satellite through the detection fence over three periods of time: July 31, 1963, to September 3, 1963, November 9, 1963, to November 15, 1963, and December 11, 1963, to February 5, 1964. The differentially corrected orbital elements discussed in Chapter I were used together with a fence crossing prediction program to calculate values of east-west and north-south angles, the rate of change of these direction cosines, and doppler frequency shift corresponding to the above mentioned observations. Because of the simplified model used in the prediction scheme, the predicted values of doppler shift were only approximate (± 30 cps). However, this model did serve as a check on the equipment, and, because of faulty digital counters and other frequency measuring devices, the percent of total observations which could be used was low. Of the 200 observations only 10 were used. This low percentage was also due to inadequate information sent from the receiver stations to NRL in several data shipments.

The basic problem of determining what effect the addition of doppler shift, measured to a given accuracy, has on the accuracy of the resulting orbital elements is primarily a theoretical one. This is true since the

present system is not equipped to measure doppler shift. The experimental "set-up" at the receiving stations was not intended to be a prototype of future doppler shift measuring equipment, but was installed solely to produce results from "raw data" which could be used to back up the theoretical results discussed in Chapter III.

Because of the large errors which exist in the measurement of rate of change of direction cosine, the errors which are generated because of the simplified prediction model can be neglected and the standard deviation (σ) of these parameters can be computed by comparing predicted and observed data. The standard deviations for all of the angle measurements have been computed by comparing system measurements with optical measurements.^{12,13}

The resolution of the experimental set-up is 10 c.p.s. in doppler shift. Hence a doppler shift sigma value of 10 c.p.s. is assumed.

For each of the 10 observations, two sets of orbital elements are generated using the method discussed in Chapter II. In one set the terms dependent on doppler shift are eliminated by using a large σ value for doppler shift. This results in a set of elements derived only from angles and rate of change of direction cosines. In the second set the doppler shift measurements are included by using a σ value of 10 c.p.s. In all runs range measurements are eliminated by using large σ values. The improvement that the addition of doppler shift has on the orbital elements can be seen by comparing both sets with the above mentioned differentially corrected set computed at the same epoch. These results are tabulated in Table I where σ_d is the standard deviation associated with doppler shift measurement. It should be pointed out that, owing to the small percent of cases with correct doppler shift measurement, the

TABLE I - Comparison Between Classical Orbital Elements Derived from Data Runs 1-10, Computed for Doppler Shift Sigma Values of 10 and 10^{21} c.p.s., and Differentially Corrected Elements

	Epoch G.M.T. (h.m.s.)	a (Mi.)	i (Deg.)	e	v (Deg.)	ω (Deg.)	Ω (Deg.)
Run 1	7/31/63						
$\sigma_d = 10^{21}$	125014.2	4973.4	47.956	0.10430	282.600	124.567	14.156
$\sigma_d = 10$		4896.5	48.107	0.05864	284.330	122.690	14.375
Diff Cor		4869.5	47.235	0.05641	280.436	131.290	13.064
Run 2	8/25/63						
$\sigma_d = 10^{21}$	063854.9	7112.9	43.292	0.36625	304.122	109.308	284.559
$\sigma_d = 10$		4545.1	46.708	0.12501	186.166	223.001	290.582
Diff Cor		4866.5	47.284	0.06071	183.012	225.532	291.056
Run 3	9/1/63						
$\sigma_d = 10^{21}$	011719.2	4580.9	76.509	0.55404	228.293	159.980	288.469
$\sigma_d = 10$		4353.3	46.789	0.15935	168.614	230.582	266.445
Diff Cor		4865.7	47.288	0.06177	148.092	250.119	268.558
Run 4	8/28/63						
$\sigma_d = 10^{21}$	033158.4	6266.2	66.750	0.55107	251.752	141.598	300.306
$\sigma_d = 10$		5745.1	51.723	0.10277	40.656	359.391	287.365
Diff Cor		4866.0	47.298	0.06155	167.338	236.220	281.549
Run 5	8/30/63						
$\sigma_d = 10^{21}$	032340.8	4694.8	49.173	0.16819	229.049	174.569	277.300
$\sigma_d = 10$		4939.0	47.263	0.03976	164.029	241.264	274.788
Diff Cor		4865.7	47.288	0.06177	161.221	244.007	274.933
Run 6	8/31/63						
$\sigma_d = 10^{21}$	022038.1	3869.6	60.298	0.49290	213.050	181.837	283.152
$\sigma_d = 10$		4163.4	46.977	0.20061	174.030	228.780	269.919
Diff Cor		4865.7	47.288	0.06177	155.058	247.063	271.745
Run 7	1/3/64						
$\sigma_d = 10^{21}$	161353.9	5342.3	48.330	0.13012	31.844	15.316	216.123
$\sigma_d = 10$		5305.3	48.357	0.10954	8.395	38.739	216.162
Diff Cor		4861.8	47.243	0.03102	22.574	25.595	214.475
Run 8	2/1/64						
$\sigma_d = 10^{21}$	143632.4	5270.6	47.802	0.08792	2.658	130.512	117.643
$\sigma_d = 10$		5195.0	47.940	0.07458	358.568	134.735	117.445
Diff Cor		4861.7	47.178	0.01587	346.953	145.789	118.556
Run 9	2/11/64						
$\sigma_d = 10^{21}$	114059.0	5242.0	47.383	0.08663	321.081	172.058	85.695
$\sigma_d = 10$		5118.2	47.575	0.04803	352.861	140.465	85.418
Diff Cor		4861.7	47.171	0.01154	301.975	190.921	85.873

TABLE I - (Continued)

	Epoch G.M.T. (h.m.s.)	a (Mi.)	i (Deg.)	e	v (Deg.)	ω (Deg.)	Ω (Deg.)
Run 10	2/11/64						
$\sigma_d = 10^{21}$	052949.0	4185.3	48.824	0.21964	147.233	259.760	89.173
$\sigma_d = 10$		4658.0	46.532	0.04891	181.688	227.635	85.713
Diff Cor		4861.7	47.171	0.01154	218.223	190.095	86.731

author was forced to use some cases in which the satellite was in an unfavorable position relative to the two receiver stations. For example, observations were used which were far east or far west of both receiver stations. In these cases the resolution of the velocity vector is more critical than for an over-head observation, and the error in rate of change of direction cosine has a greater influence on the corresponding error in velocity. The number of these cases could be reduced by extending ground coverage through the use of the two additional receiver stations mentioned in Chapter I.

It can be seen from Table I that the addition of doppler results in a marked improvement in the resulting elements. As a better means of studying this error reduction, the errors Δx , Δh , and Δt , discussed in Chapter III, are calculated from the 10 groups of data runs. For each data group two sets of the above errors are generated, one by comparing the differentially corrected elements with the elements obtained without using doppler shift data and one comparing the differentially corrected set with the elements obtained including doppler shift. There are, therefore, twenty error runs, ten producing errors when doppler shift is not considered (Case I) and ten producing errors when doppler shift is considered (Case II). These errors as mentioned above are given as a function of central angle. For a given value of central

angle, a root-mean-square value is calculated for all of the errors in Case I (Δx_{RMS1} , Δh_{RMS1} , and Δt_{RMS1}). A similar calculation is made for Case II, producing Δx_{RMS2} , Δh_{RMS2} , and Δt_{RMS2} . The values of central angle used in these calculations are: 0° , 10° , 20° , 30° , 60° , and 90° . These results are tabulated in Tables II through VII. The reduction of these errors owing to the addition of doppler shift measurements is shown in Figures 15, 16, and 17. The relationship between error reduction and central angle is also seen in these figures.

In these figures the R.M.S. errors are plotted versus central angle. The curves Δx_1 , Δh_1 , and Δt_1 refer to the errors computed in Case I (doppler shift not considered); and Δx_2 , Δh_2 , and Δt_2 refer to the errors computed in Case II (doppler shift included in computations).

TABLE II - Cross Track Error in Miles Computed from Data Runs 1-10 with Doppler Shift Measurement Not Included in the Computations (Case I), and R.M. S. Values Computed for Indicated Central Angles

Data Run	Central Angle					
	0°	10°	20°	30°	60°	90°
1	-1.08	14.45	29.08	42.48	72.75	84.59
2	-15.7	-106.1	-187.5	-259.7	-421.8	-499.2
3	105.0	592.0	923.0	1131.0	1332.0	1253.0
4	-43.0	340.0	631.0	845.0	1167.0	1207.0
5	5.30	44.2	79.6	110.5	171.0	182.5
6	81.5	297.9	461.8	575.7	696.2	629.3
7	-1.70	22.0	45.8	69.0	129.6	161.5
8	-0.29	-13.61	-26.6	-38.96	-69.28	-83.44
9	5.62	2.06	-1.49	-4.95	-14.05	-19.95
10	-0.70	36.8	74.1	109.2	182.6	190.8
R.M.S.	44.53	238.8	389.1	492.4	623.6	615.0

TABLE III - Height Error in Miles Computed From Data Runs 1-10 with Doppler Shift Measurement Not Included in the Computations (Case I), and R.M.S. Values Computed for Indicated Central Angles

Data Run	Central Angle					
	0°	10°	20°	30°	60°	90°
1	-12.8	-47.2	-76.9	-101.3	-141.7	-132.4
2	-46.0	-243.0	-387.0	-482.0	-495.0	-138.0
3	-119.0	-832.0	-1460.0	-1972.0	-2877.0	-3146.0
4	134.0	-473.0	-982.0	-1394.0	-2127.0	-2316.0
5	-21.4	-169.1	-313.7	-449.3	-762.8	-902.0
6	-166.0	-626.0	-1080.0	-1492.0	-2370.0	-2760.0
7	7.0	54.0	112.0	180.0	434.0	720.0
8	21.2	32.3	52.7	82.2	219.3	409.0
9	43.1	12.5	-8.4	-19.4	7.6	119.5
10	-24.0	93.0	176.0	219.0	97.0	-304.0
R.M.S.	80.83	375.6	675.5	927.0	1397.0	1566.0

TABLE IV - Time Error in Seconds Computed From Data Runs 1-10 with Doppler Shift Measurement Not Included in the Computations (Case I), and R.M.S. Values Computed for Indicated Central Angles

Data Run	Central Angle					
	0°	10°	20°	30°	60°	90°
1	0.3	3.8	9.8	17.6	48.9	83.0
2	5.6	39.8	85.8	139.8	314.9	449.2
3	-14.0	-62.0	-40.0	33.0	420.0	897.0
4	8.0	-11.0	20.0	88.0	414.0	808.0
5	-0.8	0.5	14.0	38.9	168.0	343.7
6	-15.0	-45.0	-31.0	22.0	337.0	761.0
7	1.7	6.4	7.2	3.2	-45.5	-163.3
8	-3.4	1.3	4.8	6.4	-6.7	-59.2
9	2.3	6.5	12.7	20.1	41.8	47.5
10	6.6	-17.2	-50.0	-88.3	-199.3	-236.9
R.M.S.	7.62	28.23	36.54	62.40	251.9	495.2

TABLE V - Cross Track Error in Miles Computed From Data Runs 1-10 with Doppler Shift Measurement Included in the Computations (Case II), and R.M.S. Values Computed for Indicated Central Angles

Data Run	Central Angle					
	0°	10°	20°	30°	60°	90°
1	-1.1	17.8	35.8	52.4	90.5	105.2
2	-18.21	-27.63	-36.04	-43.1	-54.33	-50.14
3	78.1	56.6	32.9	8.20	-61.0	-105.2
4	-33.8	67.6	169.6	269.7	528.7	663.9
5	5.119	3.573	1.922	0.225	-4.569	-7.899
6	67.31	49.37	29.56	8.91	-47.88	-82.79
7	-1.7	22.4	46.1	69.0	126.9	156.4
8	-0.4	-16.6	-32.4	-47.4	-83.8	-100.2
9	5.68	-2.04	-9.69	-17.07	-35.73	-45.66
10	0.9	-13.57	-27.58	-40.65	-70.21	-79.86
R.M.S.	34.88	35.03	61.10	92.97	180.6	227.0

TABLE VI - Height Error in Miles Computed From Data Runs 1-10 with Doppler Shift Measurement Included in the Computations (Case II), and R.M.S. Values Computed from Indicated Central Angles

Data Run	Central Angle					
	0°	10°	20°	30°	60°	90°
1	-12.83	-12.46	-11.08	-8.76	2.91	19.68
2	-52.0	-67.8	-94.5	-130.4	-271.1	-415.7
3	-86.3	-95.3	-124.0	-171.0	-389.5	-637.0
4	114.0	170.0	245.0	339.0	711.0	1140.0
5	-21.0	-28.0	-31.3	-30.7	-7.10	40.2
6	-142.0	-160.0	-206.0	-277.0	-584.0	-904.0
7	7.20	14.5	31.8	59.1	198.5	408.0
8	21.1	26.7	40.1	61.0	164.6	313.7
9	42.6	48.8	60.6	77.7	156.3	261.4
10	-19.7	-17.8	-22.2	-32.7	-95.2	-185.8
R.M.S.	68.28	85.29	116.0	159.1	342.3	553.6

TABLE VII - Time Error in Seconds Computed From Data Runs 1-10 with Doppler Shift Measurement Included in the Computations (Case II), and R.M.S. Values Computed for Indicated Central Angles

Data Run	Central Angle					
	0°	10°	20°	30°	60°	90°
1	0.28	1.7	3.04	4.22	6.24	4.99
2	6.6	2.8	1.0	1.80	25.9	84.5
3	-9.7	-16.6	-21.9	-24.0	2.5	88.0
4	6.0	10.0	9.0	1.0	-79.0	-264.0
5	-0.7	3.19	7.52	11.96	22.72	24.28
6	-12.1	-20.4	-25.9	-26.2	19.9	144.0
7	1.7	7.7	12.7	16.1	9.0	-40.1
8	-3.4	0.3	3.4	5.1	-2.9	-41.3
9	2.3	3.4	3.8	3.1	-9.6	-44.4
10	6.1	3.1	0.3	-2.0	-0.6	19.4
R.M.S.	6.15	9.45	12.2	13.1	28.4	105.6

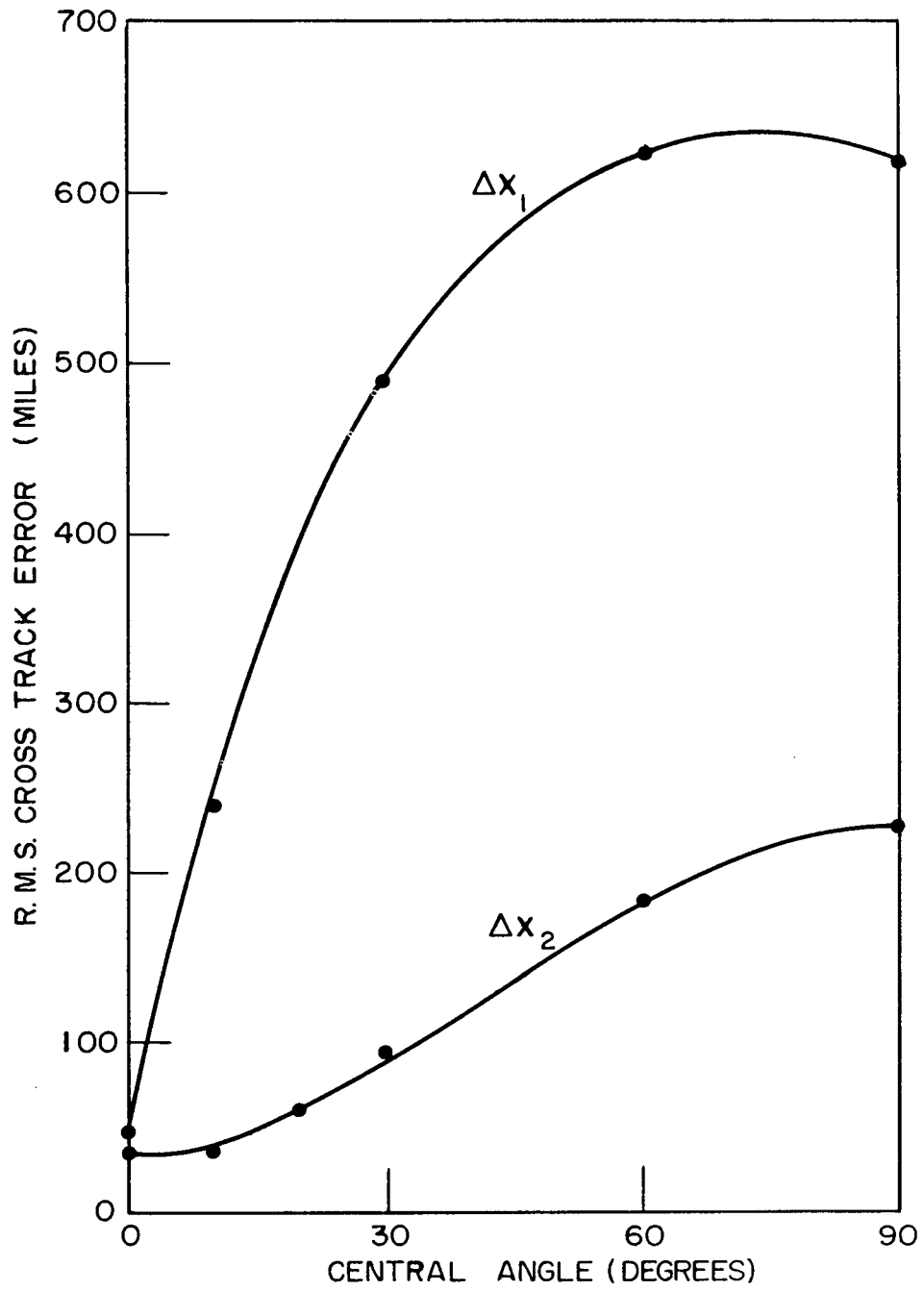


Figure 15 - Relation Between Experimental R.M.S. Cross Track Error and Central Angle for Case I and Case II

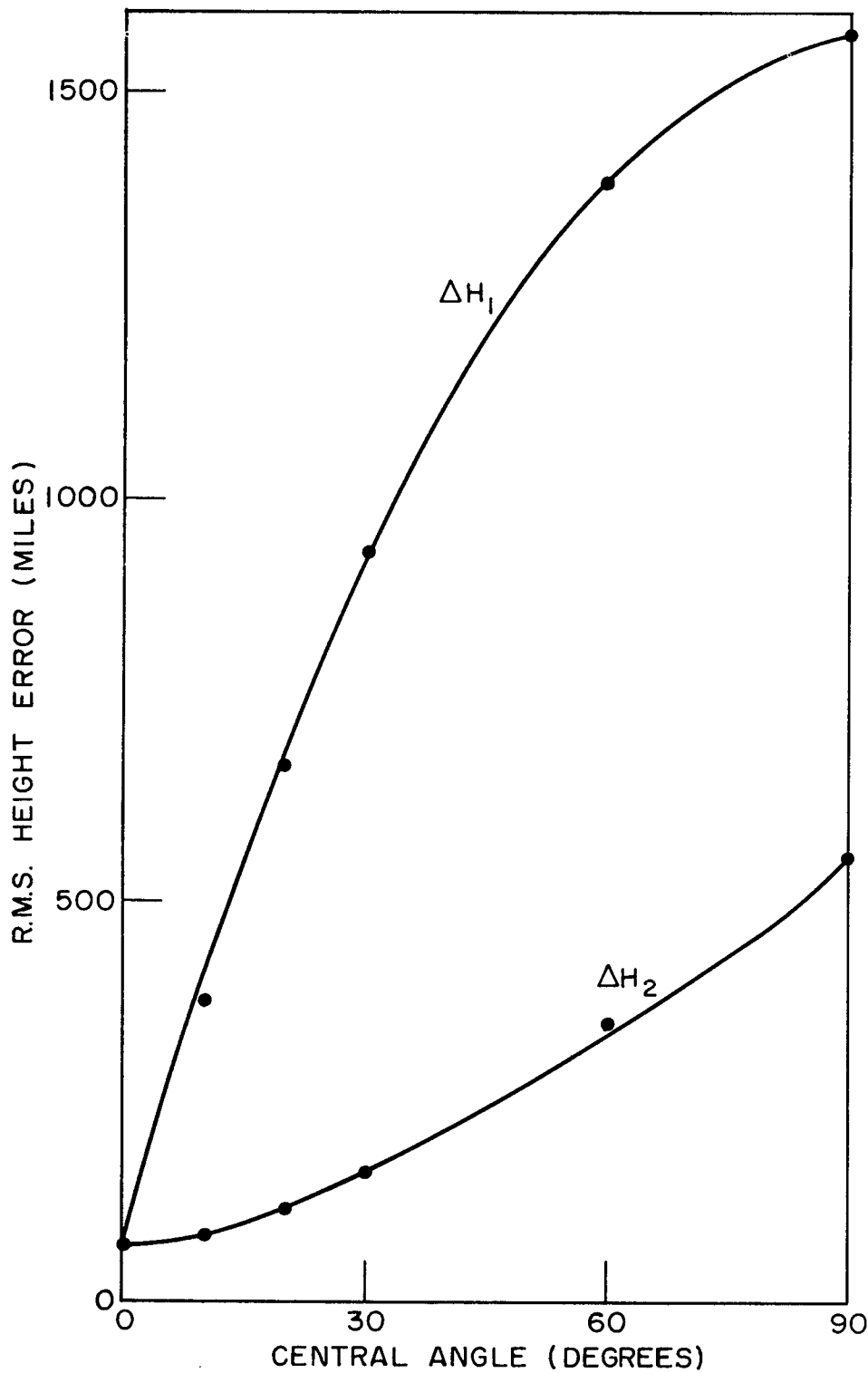


Figure 16 - Relation Between Experimental R.M.S. Height Error and Central Angle for Case I and Case II

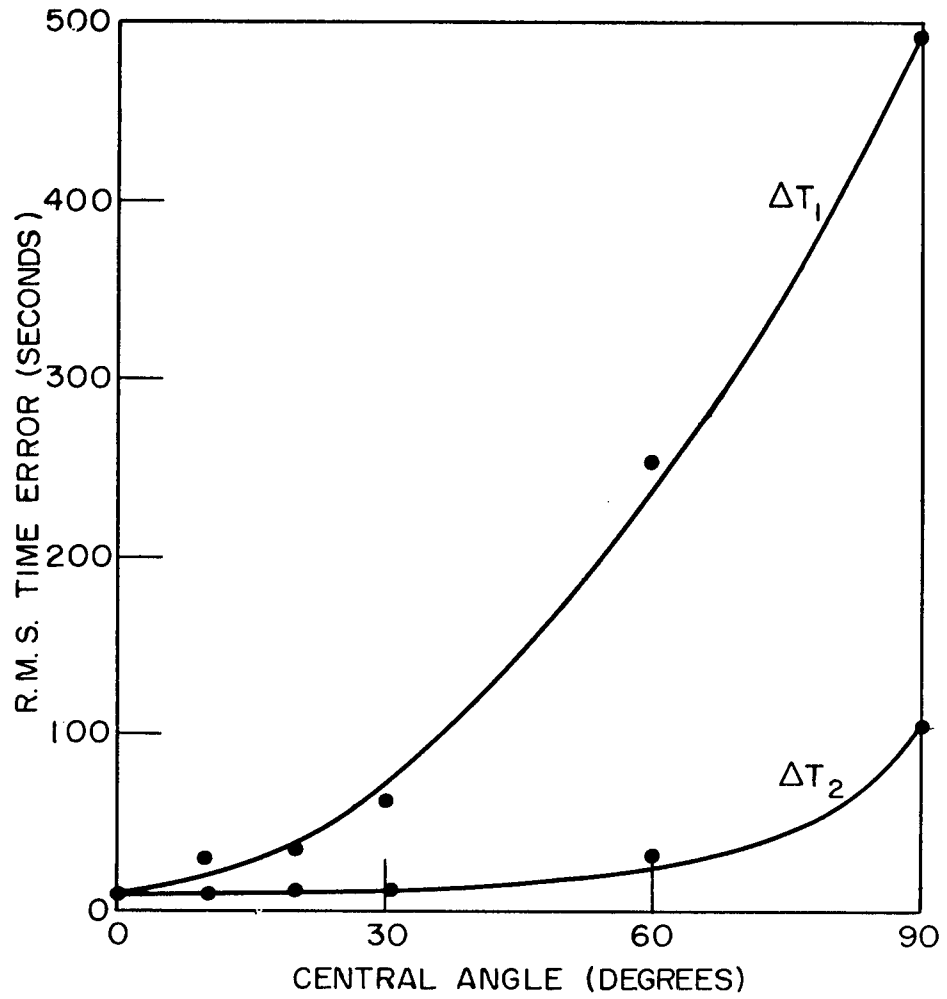


Figure 17 - Relation Between Experimental R.M.S. Time Error and Central Angle for Case I and Case II

APPENDIX A

COORDINATE TRANSFORMATIONS

The first transformation performed in the development is a time dependent rotation which transforms the coordinate system from the earth-fixed system discussed in Chapter I (x, y, z) to one in which the orbital plane is fixed (x', y', z'). This new set is an inertial set in fixed star space. This transformation, therefore, must consider the rotation of the earth in fixed star space, that is, a rotation about the earth's polar axis of 15.04106861 degrees per hour. In addition the motion of the orbital plane in fixed star space must be considered. Because of the model chosen in this work, the motion of the orbital plane in fixed star space is the rate of change of right ascension of the ascending node ($\dot{\Omega}$). This rotation is also about the earth's polar axis; hence the two rotations can be combined into one transformation. The transformation equations are given by

$$\left. \begin{aligned} x' &= x \cos \alpha t - y \sin \alpha t \\ y' &= x \sin \alpha t + y \cos \alpha t \\ z' &= z \end{aligned} \right\} \quad (32)$$

where t is time measured after epoch time and

$$\alpha = \frac{\pi}{180} (15.04106861 + \dot{\Omega}) \text{ rad/hr.}$$

The first order secular term in the Ω expansion is used in the evaluation of $\dot{\Omega}$ and is given by the expression

$$\dot{\Omega} = 0.41498 \left[\frac{r_e}{a} \right]^{7/2} \frac{\cos i}{(1 - e^2)^2} \text{ deg./hr. ,}$$

where r_e is the radius of the earth and the remaining elements are found in Chapter II.

The velocity transformation equations can be obtained by differentiating equations (32) and are given by

$$\left. \begin{aligned} \dot{x}' &= \dot{x} \cos \alpha t - \alpha x \sin \alpha t - \dot{y} \sin \alpha t \\ &\quad - \alpha y \cos \alpha t \\ \dot{y}' &= \dot{x} \sin \alpha t + \alpha x \cos \alpha t + \dot{y} \cos \alpha t - \alpha y \sin \alpha t \\ \dot{z}' &= \dot{z} \end{aligned} \right\} \quad (33)$$

In the development in Chapter II, the transformation is made at epoch time. Hence $t = 0$ and equations (32) and (33) become

$$\begin{aligned} x' &= x, \\ y' &= y, \\ z' &= z, \end{aligned}$$

and

$$\begin{aligned} \dot{x}' &= \dot{x} - \alpha y, \\ \dot{y}' &= \dot{y} + \alpha x, \\ \dot{z}' &= \dot{z} . \end{aligned}$$

After the above transformation is performed inclination (i) and longitude of the ascending node (λ_N) are computed in the inertial frame and the two following coordinate rotations are made which transform the orbital plane into the x, y plane. The first of these is a rotation about z' producing a set (x_N, y_N, z_N) whose positive x axis lies along the line of nodes and points in the direction of the ascending node. The transformation equations for the position vector to the satellite are

$$\left. \begin{aligned} x_N &= x' \cos \lambda_N - y' \sin \lambda_N, \\ y_N &= x' \sin \lambda_N + y' \cos \lambda_N, \\ z_N &= z' \end{aligned} \right\} \quad (34)$$

The transformation equations for the velocity vector are obtained by taking the derivatives of equations (34) with respect to time and are

$$\dot{x}_N = \dot{x}' \cos \lambda_N - \dot{y}' \sin \lambda_N,$$

$$\dot{y}_N = \dot{x}' \sin \lambda_N + \dot{y}' \cos \lambda_N,$$

$$\dot{z}_N = \dot{z}'.$$

The set (x'', y'', z'') , which has its x'', y'' plane coinciding with the orbital plane, is obtained by rotating about x_N through the angle i (inclination angle). The position and velocity transformation equations for this rotation are

$$x'' = x_N,$$

$$y'' = y_N \cos i + z_N \sin i,$$

$$z'' = -y_N \sin i + z_N \cos i,$$

and

$$\dot{x}'' = \dot{x}_N,$$

$$\dot{y}'' = \dot{y}_N \cos i + \dot{z}_N \sin i,$$

$$\dot{z}'' = -\dot{y}_N \sin i + \dot{z}_N \cos i.$$

The final transformation is a time dependent rotation from the (x'', y'', z'') set to a set in which the ellipse is fixed in the x, y plane $(\bar{x}, \bar{y}, \bar{z})$. The rate of change of argument of perigee ($\dot{\omega}$) is the

angular rotation of the ellipse in the orbital plane. Hence this transformation is a rotation about the z'' axis having the transformation equations

$$\left. \begin{aligned} \bar{x} &= x'' \cos \dot{\omega}t - y'' \sin \dot{\omega}t, \\ \bar{y} &= x'' \sin \dot{\omega}t + y'' \cos \dot{\omega}t, \\ \bar{z} &= z'', \end{aligned} \right\} \quad (35)$$

$$\left. \begin{aligned} \dot{\bar{x}} &= \dot{x}'' \cos \dot{\omega}t - \dot{\omega}x'' \sin \dot{\omega}t - \dot{y}'' \sin \dot{\omega}t \\ &\quad - \dot{\omega}y'' \cos \dot{\omega}t, \\ \dot{\bar{y}} &= \dot{x}'' \sin \dot{\omega}t + \dot{\omega}x'' \cos \dot{\omega}t + \dot{y}'' \cos \dot{\omega}t \\ &\quad - \dot{\omega}y'' \sin \dot{\omega}t, \\ \dot{\bar{z}} &= \dot{z}'' \end{aligned} \right\} \quad (36)$$

The first order secular term in the argument of perigee (ω) expansion is used in the evaluation of $\dot{\omega}$ and is given by the expression

$$\dot{\omega} = -0.20749 \left[\frac{r_e}{a} \right]^{7/2} \frac{\pi}{180} \frac{(5 \cos^2 i - 1)}{(1 - e^2)^2} \text{ rad/hr.}$$

As was the case with the first transformation discussed above, this transformation is made at epoch time. Hence $t = 0$ and equations (35) and (36) become

$$\begin{aligned} \bar{x} &= x'', \\ \bar{y} &= y'', \\ \bar{z} &= z'', \end{aligned}$$

$$\dot{\bar{x}} = \dot{x}'' - \dot{\omega}y'',$$

$$\dot{\bar{y}} = \dot{y}'' + \dot{\omega}x'',$$

$$\dot{\bar{z}} = \dot{z}'' .$$

SELECTED BIBLIOGRAPHY

1. P. J. Klass, Spasur Net Giving Vital Norad Coverage, Aviation Week & Space Technology, 77, Number 22 (1962).
2. R. L. Easton and J. J. Fleming, The Navy Space Surveillance System, Proceedings of the I.R.E., 48, 663 (1960).
3. D. W. Lynch, Navy's Space Surveillance System's Two-Point Orbits, N.R.L. Report 6072, U.S. Naval Research Laboratory, Washington, D.C., (March 1964).
4. D. Brouwer and G. M. Clemence, Methods of Celestial Mechanics (Academic Press, New York and London, 1961), Page 213.
5. R. W. Wolverton, Flight Performance Handbook for Orbital Operations (John Wiley and Sons, Inc., New York and London, 1963), Chapter 2.
6. S. W. McCuskey, Introduction to Celestial Mechanics (Addison-Wesley Publishing Company, Inc., Reading, Massachusetts, Palo Alto, and London, 1963), Page 169.
8. P. Herget, The Computation of Orbits (Published Privately by P. Herget, University of Cincinnati, Cincinnati, Ohio, 1948), Page 27.
10. P. Herget, *ibid.*, Page 29.
11. S. W. McCuskey, *op. cit.*, Page 27.
12. L. O. Hayden, Optical Calibration of the U.S. Naval Space Surveillance System, N.R.L. Report 5741, U.S. Naval Research Laboratory Washington, D.C., (March 1962).

Unpublished Materials

7. P. Musen, Class Notes from Introduction to Celestial Mechanics, University of Maryland, College Park, Maryland.
9. P. Musen, *ibid.*
13. L. O. Hayden and T. B. McCaskill, Optical Calibration of the Silver Lake Space Surveillance Station, Space Surveillance Branch Technical Memorandum No. 108, U.S. Naval Research Laboratory, Washington, D.C., (April, 1964).

DOCUMENT CONTROL DATA - R&D

(Security classification of title, body of abstract and indexing annotation must be entered when the overall report is classified)

1. ORIGINATING ACTIVITY (Corporate author) U.S. Naval Research Laboratory Washington, D.C. - 20390		2a. REPORT SECURITY CLASSIFICATION UNCLASSIFIED	
		2b. GROUP	
3. REPORT TITLE The Computation of Optimum Orbital Elements Derived from a Single Coincident Observation by Two Receiving Stations of the Naval Space Surveillance System			
4. DESCRIPTIVE NOTES (Type of report and inclusive dates) This is an interim report on one phase of the problem.			
5. AUTHOR(S) (Last name, first name, initial) deVezin, Howard G., Jr.			
6. REPORT DATE October 22, 1964		7a. TOTAL NO. OF PAGES 72	7b. NO. OF REFS 13
8a. CONTRACT OR GRANT NO. NRL Problem R02-35		9a. ORIGINATOR'S REPORT NUMBER(S) NRL Report 6172	
b. PROJECT NO. RT 8801-001/652-1/S434-00-01		9b. OTHER REPORT NO(S) (Any other numbers that may be assigned this report)	
c.			
d.			
10. AVAILABILITY/LIMITATION NOTICES Unlimited availability			
11. SUPPLEMENTARY NOTES		12. SPONSORING MILITARY ACTIVITY Navy Department (Bureau of Naval Weapons)	
13. ABSTRACT This thesis is concerned with an investigation into a method of determining the orbital elements of a passive artificial earth satellite using information obtained from a single coincident satellite observation of short time duration. This information is obtained from two receiving stations of the U.S. Naval Space Surveillance System, a C.W. radar network of three transmitting stations and four receiving stations which sets up an electronic "fence" stretching across the southern United States. A list of the information given by two receiving stations is as follows: two east-west angles (angles measured in the plane of the detection "fence"), two north-south angles (angles measured normal to the plane of the detection "fence"), rate of change of east-west direction cosine measured by both stations, and rate of change of north-south direction cosine measured by both stations. In addition the system can be adapted to measure the doppler frequency shift from one of the three transmitters to the receiver station and the distance from one of the three transmitters to the satellite to the receiver station (bi-static range). All of this information results in redundant data (i.e. more data than are needed to determine the orbit of the satellite). In addition, owing to inaccuracies of the system and owing to noise, different groupings of the information will produce different values of orbital parameters; hence in general the information is inconsistent.			

UNCLASSIFIED

14. KEY WORDS	LINK A		LINK B		LINK C	
	ROLE	WT	ROLE	WT	ROLE	WT
Theory Analysis of satellite data Determination of satellite orbits Computation of orbital elements Space Surveillance System Single coincident satellite observation East-west angles North-south angles Doppler frequency shift Optimum values from redundant data Error analysis Least squares fit						

INSTRUCTIONS

1. **ORIGINATING ACTIVITY:** Enter the name and address of the contractor, subcontractor, grantee, Department of Defense activity or other organization (*corporate author*) issuing the report.

2a. **REPORT SECURITY CLASSIFICATION:** Enter the overall security classification of the report. Indicate whether "Restricted Data" is included. Marking is to be in accordance with appropriate security regulations.

2b. **GROUP:** Automatic downgrading is specified in DoD Directive 5200.10 and Armed Forces Industrial Manual. Enter the group number. Also, when applicable, show that optional markings have been used for Group 3 and Group 4 as authorized.

3. **REPORT TITLE:** Enter the complete report title in all capital letters. Titles in all cases should be unclassified. If a meaningful title cannot be selected without classification, show title classification in all capitals in parenthesis immediately following the title.

4. **DESCRIPTIVE NOTES:** If appropriate, enter the type of report, e.g., interim, progress, summary, annual, or final. Give the inclusive dates when a specific reporting period is covered.

5. **AUTHOR(S):** Enter the name(s) of author(s) as shown on or in the report. Enter last name, first name, middle initial. If military, show rank and branch of service. The name of the principal author is an absolute minimum requirement.

6. **REPORT DATE:** Enter the date of the report as day, month, year, or month, year. If more than one date appears on the report, use date of publication.

7a. **TOTAL NUMBER OF PAGES:** The total page count should follow normal pagination procedures, i.e., enter the number of pages containing information.

7b. **NUMBER OF REFERENCES:** Enter the total number of references cited in the report.

8a. **CONTRACT OR GRANT NUMBER:** If appropriate, enter the applicable number of the contract or grant under which the report was written.

8b, 8c, & 8d. **PROJECT NUMBER:** Enter the appropriate military department identification, such as project number, subproject number, system numbers, task number, etc.

9a. **ORIGINATOR'S REPORT NUMBER(S):** Enter the official report number by which the document will be identified and controlled by the originating activity. This number must be unique to this report.

9b. **OTHER REPORT NUMBER(S):** If the report has been assigned any other report numbers (*either by the originator or by the sponsor*), also enter this number(s).

10. **AVAILABILITY/LIMITATION NOTICES:** Enter any limitations on further dissemination of the report, other than those

imposed by security classification, using standard statements such as:

- (1) "Qualified requesters may obtain copies of this report from DDC."
- (2) "Foreign announcement and dissemination of this report by DDC is not authorized."
- (3) "U. S. Government agencies may obtain copies of this report directly from DDC. Other qualified DDC users shall request through _____."
- (4) "U. S. military agencies may obtain copies of this report directly from DDC. Other qualified users shall request through _____."
- (5) "All distribution of this report is controlled. Qualified DDC users shall request through _____."

If the report has been furnished to the Office of Technical Services, Department of Commerce, for sale to the public, indicate this fact and enter the price, if known.

11. **SUPPLEMENTARY NOTES:** Use for additional explanatory notes.

12. **SPONSORING MILITARY ACTIVITY:** Enter the name of the departmental project office or laboratory sponsoring (*paying for*) the research and development. Include address.

13. **ABSTRACT:** Enter an abstract giving a brief and factual summary of the document indicative of the report, even though it may also appear elsewhere in the body of the technical report. If additional space is required, a continuation sheet shall be attached.

It is highly desirable that the abstract of classified reports be unclassified. Each paragraph of the abstract shall end with an indication of the military security classification of the information in the paragraph, represented as (TS), (S), (C), or (U).

There is no limitation on the length of the abstract. However, the suggested length is from 150 to 225 words.

14. **KEY WORDS:** Key words are technically meaningful terms or short phrases that characterize a report and may be used as index entries for cataloging the report. Key words must be selected so that no security classification is required. Identifiers, such as equipment model designation, trade name, military project code name, geographic location, may be used as key words but will be followed by an indication of technical context. The assignment of links, roles, and weights is optional.

DOCUMENT CONTROL DATA - R&D
(Continuation Sheet)

NRL Report 6172

UNCLASSIFIED

UNCLASSIFIED

13.

The purpose of this thesis is to arrive at a method of computing orbital elements using all of the information that the system does measure or can be adapted to measure. This method would introduce weighting factors determined, for example, by the accuracy with which the system can measure the parameter in question. This method is then used to study the effect that the addition of doppler shift and bi-static range measurements have on the accuracy of the resulting orbital elements.